8. Russell DG. *Mycobacterium tuberculosis*: here today, and here tomorrow. Nat Rev Mol Cell Biol 2001;2:569–577.
9. Rink J, Ghigo E, Kalaidzidis Y, Zerial M. Rab conversion as a mechanism of progression from early to late endosomes. Cell 2005;122: 735–749.
10. Vergne I, Chua J, Singh SB, Deretic V. Cell biology of *Mycobacterium tuberculosis* phagosome. Annu Rev Cell Dev Biol 2004;20:367–394.
11. Deretic V, Vergne I, Chua J, Master S, Singh SB, Fazio JA, Kyei G. Endosomal membrane traffic: convergence point targeted by *Mycobacterium tuberculosis* and HIV. Cell Microbiol 2004;6: 999–1009.
12. Roberts EA, Chua J, Kyei GB, Deretic V. Higher order Rab programming in phagolysosome biogenesis. J Cell Biol 2006;174:923–929.
13. Vergne I, Chua J, Lee HH, Lucas M, Belisle J, Deretic V. Mechanism of phagolysosome biogenesis block by viable *Mycobacterium tuberculosis*. Proc Natl Acad Sci U S A 2005;102:4033–4038.
14. Via LE, Deretic D, Ulmer RJ, Hibler NS, Huber LA, Deretic V. Arrest of mycobacterial phagosome maturation is caused by a block in vesicle fusion between stages controlled by rab5 and rab7. J Biol Chem 1997;272:13326–13331.
15. Kelley VA, Schorey JS. *Mycobacterium's* arrest of phagosome maturation in macrophages requires Rab5 activity and accessibility to iron. Mol Biol Cell 2003;14:3366–3377.
16. Sun J, Deghmane AE, Soualhine H, Hong T, Bucci C, Solodkin A, Hmama Z. *Mycobacterium bovis* BCG disrupts the interaction of Rab7 with RILP contributing to inhibition of phagosome maturation. J Leukoc Biol 2007;82:1437–1445.
17. Seto S, Matsumoto S, Ohta I, Tsujimura K, Koide Y. Dissection of Rab7 localization on *Mycobacterium tuberculosis* phagosome. Biochem Biophys Res Commun 2009;387:272–277.
18. Seto S, Matsumoto S, Tsujimura K, Koide Y. Differential recruitment of CD63 and Rab7-interacting-lysosomal-protein to phagosomes containing *Mycobacterium tuberculosis* in macrophages. Microbiol Immunol 2010;54:170–174.
19. Kyei GB, Vergne I, Chua J, Roberts E, Harris J, Junutula JR, Deretic V. Rab14 is critical for maintenance of *Mycobacterium tuberculosis* phagosome maturation arrest. EMBO J 2006;25:5250–5259.
20. Schwartz SL, Cao C, Pylypenko O, Rak A, Wandinger-Ness A. Rab GTPases at a glance. J Cell Sci 2007;120:3905–3910.
21. Stenmark H, Olkkonen VM. The Rab GTPase family. Genome Biol 2001;2:REVIEWS3007.
22. Garin J, Diez R, Kieffer S, Dermine JF, Duclos S, Gagnon E, Sadoul R, Rondeau C, Desjardins M. The phagosome proteome: insight into phagosome functions. J Cell Biol 2001;152:165–180.
23. Rogers LD, Foster LJ. The dynamic phagosomal proteome and the contribution of the endoplasmic reticulum. Proc Natl Acad Sci U S A 2007;104:18520–18525.
24. Shui W, Sheu L, Liu J, Smart B, Petzold CJ, Hsieh TY, Pitcher A, Keasling JD, Bertozzi CR. Membrane proteomics of phagosomes suggests a connection to autophagy. Proc Natl Acad Sci U S A 2008;105:16952–16957.
25. Smith AC, Heo WD, Braun V, Jiang X, Macrae C, Casanova JE, Scidmore MA, Grinstein S, Meyer T, Brumell JH. A network of Rab GTPases controls phagosome maturation and is modulated by *Salmonella enterica* serovar Typhimurium. J Cell Biol 2007;176:263–268.
26. Beatty WL, Rhoades ER, Hsu DK, Liu FT, Russell DG. Association of a macrophage galactoside-binding protein with *Mycobacterium*-containing phagosomes. Cell Microbiol 2002;4:167–176.
27. Desjardins M, Huber LA, Parton RG, Griffiths G. Biogenesis of phagolysosomes proceeds through a sequential series of interactions with the endocytic apparatus. J Cell Biol 1994;124:677–688.
28. Brumell JH, Scidmore MA. Manipulation of rab GTPase function by intracellular bacterial pathogens. Microbiol Mol Biol Rev 2007;71:636–652.
29. Clemens DL, Lee BY, Horwitz MA. *Mycobacterium tuberculosis* and *Legionella pneumophila* phagosomes exhibit arrested maturation despite acquisition of Rab7. Infect Immun 2000;68:5154–5166.
30. Fratti RA, Backer JM, Gruenberg J, Corvera S, Deretic V. Role of phosphatidylinositol 3-kinase and Rab5 effectors in phagosomal biogenesis and mycobacterial phagosome maturation arrest. J Cell Biol 2001;154:631–644.
31. Ng EL, Wang Y, Tang BL. Rab22B's role in trans-Golgi network membrane dynamics. Biochem Biophys Res Commun 2007;361:751–757.
32. Wang T, Hong W. Interorganellar regulation of lysosome positioning by the Golgi apparatus through Rab34 interaction with Rab-interacting lysosomal protein. Mol Biol Cell 2002;13:4317–4332.
33. Wasmeier C, Romao M, Plowright L, Bennett DC, Raposo G, Seabra MC. Rab38 and Rab32 control post-Golgi trafficking of melanogenic enzymes. J Cell Biol 2006;175:271–281.
34. Ullrich HJ, Beatty WL, Russell DG. Direct delivery of procathepsin D to phagosomes: implications for phagosome biogenesis and parasitism by *Mycobacterium*. Eur J Cell Biol 1999;78:739–748.
35. Dejgaard SY, Murshid A, Erman A, Kizilay O, Verbich D, Lodge R, Dejgaard K, Ly-Hartig TB, Pepperkok R, Simpson JC, Presley JF. Rab18 and Rab43 have key roles in ER-Golgi trafficking. J Cell Sci 2008;121:2768–2781.
36. Das Sarma J, Kaplan BE, Willemsen D, Koval M. Identification of rab20 as a potential regulator of connexin 43 trafficking. Cell Commun Adhes 2008;15:65–74.
37. Curtis LM, Gluck S. Distribution of Rab GTPases in mouse kidney and comparison with vacuolar H+-ATPase. Nephron Physiol 2005;100:31–42.
38. Lee BY, Jethwaney D, Schilling B, Clemens DL, Gibson BW, Horwitz MA. The *Mycobacterium bovis* bacille Calmette-Guerin phagosome proteome. Mol Cell Proteomics 2010;9:32–53.
39. Philips JA, Porto MC, Wang H, Rubin EJ, Perrimon N. ESCRT factors restrict mycobacterial growth. Proc Natl Acad Sci U S A 2008;105:3070–3075.
40. Kumar D, Nath L, Kamal MA, Varshney A, Jain A, Singh S, Rao KV. Genome-wide analysis of the host intracellular network that regulates survival of *Mycobacterium tuberculosis*. Cell 2010;140:731–743.
41. Vanlandingham PA, Ceresa BP. Rab7 regulates late endocytic trafficking downstream of multivesicular body biogenesis and cargo sequestration. J Biol Chem 2009;284:12110–12124.
42. Vergne I, Fratti RA, Hill PJ, Chua J, Belisle J, Deretic V. *Mycobacterium tuberculosis* phagosome maturation arrest: mycobacterial phosphatidylinositol analog phosphatidylinositol mannoside stimulates early endosomal fusion. Mol Biol Cell 2004;15:751–760.
43. Cox D, Lee DJ, Dale BM, Calafat J, Greenberg S. A Rab11-containing rapidly recycling compartment in macrophages that promotes phagocytosis. Proc Natl Acad Sci U S A 2000;97:680–685.
44. Frigui W, Bottai D, Majlessi L, Monot M, Josselin E, Brodin P, Garnier T, Gicquel B, Martin C, Leclerc C, Cole ST, Brosch R. Control of *M. tuberculosis* ESAT-6 secretion and specific T cell recognition by PhoP. PLoS Pathog 2008;4:e33.
45. Abdallah AM, Gey van Pittius NC, Champion PA, Cox J, Luirink J, Vandenbroucke-Grauls CM, Appelmelk BJ, Bitter W. Type VII secretion – mycobacteria show the way. Nat Rev Microbiol 2007;5: 883–891.
46. Smith J, Manoranjan J, Pan M, Bohsali A, Xu J, Liu J, McDonald KL, Szyk A, LaRonde-LeBlanc N, Gao LY. Evidence for pore formation in host cell membranes by ESX-1-secreted ESAT-6 and its role in *Mycobacterium marinum* escape from the vacuole. Infect Immun 2008;76:5478–5487.
47. Cardoso CM, Jordao L, Vieira OV. Rab10 regulates phagosome maturation and its overexpression rescues *Mycobacterium*-containing phagosomes maturation. Traffic 2010;11:221–235.
48. Aoki K, Matsumoto S, Hirayama Y, Wada T, Ozeki Y, Niki M, Domenech P, Umemori K, Yamamoto S, Mineda A, Matsumoto M, Kobayashi K. Extracellular mycobacterial DNA-binding protein 1 participates in mycobacterium-lung epithelial cell interaction through hyaluronic acid. J Biol Chem 2004;279:39798–39806.
49. Chua J, Deretic V. *Mycobacterium tuberculosis* reprograms waves of phosphatidylinositol 3-phosphate on phagosomal organelles. J Biol Chem 2004;279:36982–36992.
50. Fukuda M, Kanno E, Ishibashi K, Itoh T. Large scale screening for novel rab effectors reveals unexpected broad Rab binding specificity. Mol Cell Proteomics 2008;7:1031–1042.
51. Itoh T, Satoh M, Kanno E, Fukuda M. Screening for target Rabs of TBC (Tre-2/Bub2/Cdc16) domain-containing proteins based on their Rab-binding activity. Genes Cells 2006;11:1023–1037.

Biochemical and Biophysical Research Communications 410 (2011) 371–375

Contents lists available at ScienceDirect

Biochemical and Biophysical Research Communications

journal homepage: www.elsevier.com/locate/ybbrc

Mobility of late endosomal and lysosomal markers on phagosomes analyzed by fluorescence recovery after photobleaching

Keiko Sugaya [a], Shintaro Seto [b,*], Kunio Tsujimura [b], Yukio Koide [b,c]

[a] Department of Health Science, Hamamatsu University School of Medicine, 1-20-1 Handa-yama, Higashi-ku, Hamamatsu 431-3192, Japan
[b] Department of Infectious Diseases, Hamamatsu University School of Medicine, 1-20-1 Handa-yama, Higashi-ku, Hamamatsu 431-3192, Japan
[c] Hamamatsu University School of Medicine, 1-20-1 Handa-yama, Higashi-ku, Hamamatsu 431-3192, Japan

ARTICLE INFO

Article history:
Received 30 May 2011
Available online 12 June 2011

Keywords:
Fluorescence recovery after photobleaching
IFN-γ
LAMP1
Mycobacterium bovis BCG
Phagosome
Rab7

ABSTRACT

During phagosome maturation, the late endosomal marker Rab7 and the lysosomal marker LAMP1 localize to the phagosomes. We investigated the mobility of Rab7 and LAMP1 on the phagosomes in macrophages by fluorescence recovery after photobleaching (FRAP) analysis. Rab7 was mobile between the phagosomal membrane and the cytosol in macrophages that ingested latex beads during phagosome maturation. The addition of interferon-γ (IFN-γ) restricted this mobility, suggesting that Rab7 is forced to bind to the phagosomal membrane by IFN-γ-mediated activation. Immobilization of LAMP1 on the phagosomes was observed irrespective of IFN-γ-activation. We further examined the mobility of Rab7 on the phagosomes containing *Mycobacterium bovis* BCG by FRAP analysis. The rate of fluorescence recovery for Rab7 on mycobacterial phagosomes was lower than that on the phagosomes containing latex beads, suggesting that mycobacteria impaired the mobility of Rab7 and arrested phagosome maturation.

1. Introduction

Innate immunity provides the first line of defense against infection, and phagocytosis is an important step in the innate immune response. Pathogens phagocytosed by macrophages are enclosed into phagosomes, which interact with early and late endosomal vesicles. During this process, known as phagosome maturation, phagosomes acquire degradative and microbicidal properties and undergo phagolysosome biogenesis by fusing with lysosomes. Several proteins, including Rab GTPase proteins, play pivotal roles in phagosome maturation and phagolysosome biogenesis [1]. Rab5 is associated with early phagosomes followed by recruitment of its effector proteins, EEA1 and Class III phosphatidylinositol 3-kinase [2]. Rab7 appears on the phagosome membrane after Rab5 dissociation and resides there during phagosome maturation [3]. Rab7 regulates the transportation and fusion of late endosomes and lysosomes [1]. As an example, Rab7-interacting-lysosomal protein (RILP), an effector protein of Rab7, recruits the minus-end motor complex dynein–dynactin to the phagosome, resulting in migration of the phagosomes to the microtubule-organizing center where late endosomal and lysosomal compartments accumulate [4]. Lysosomal-associated membrane protein 1 (LAMP1) and LAMP2, the major components of lysosomes, accumulate in phagolysosomes via the fusion of lysosomes with the phagosome [5]. Although Rab7, LAMP1 and LAMP2 have important roles in the process of phagosome maturation and phagolysosome biogenesis [1,6], the accumulation kinetics of these late endosomal and lysosomal markers is not yet fully understood.

Mycobacterium tuberculosis is the causative agent of tuberculosis and has the ability to survive and replicate in macrophages. It is long believed that *M. tuberculosis* causes the arrest of phagosome maturation during Rab5–Rab7 conversion [7,8] and survives within infected macrophages. However, Sun et al. [9] reported that Rab7 localizes to the phagosomes containing *Mycobacterium bovis* BCG. We recently reported that Rab7 is transiently recruited to and subsequently released from the phagosomes containing *M. tuberculosis* using imaging and biochemical analyses [10,11]. Evidence regarding Rab7 localization to mycobacterial phagosomes is accumulating; however, detailed localization kinetics remain to be elucidated.

To understand the localization kinetics of Rab7 and LAMP1 to the phagosome membrane, we employed fluorescence recovery after photobleaching (FRAP) analysis and chased their mobility on the phagosomes in macrophages during phagosome maturation in the presence and absence of interferon (IFN)-γ. We further examine the mobility of Rab7 on the phagosomes containing *M. bovis* BCG.

2. Materials and methods

2.1. Cell and bacterial cultures

Raw264.7 macrophages were obtained from the American Type Culture Collection and maintained in Dulbecco's modified Eagle's medium (DMEM) supplemented with 10% foetal bovine serum

* Corresponding author. Fax: +81 53 435 2335.
E-mail address: s-seto@hama-med.ac.jp (S. Seto).

0006-291X/$ - see front matter © 2011 Elsevier Inc. All rights reserved.
doi:10.1016/j.bbrc.2011.06.023

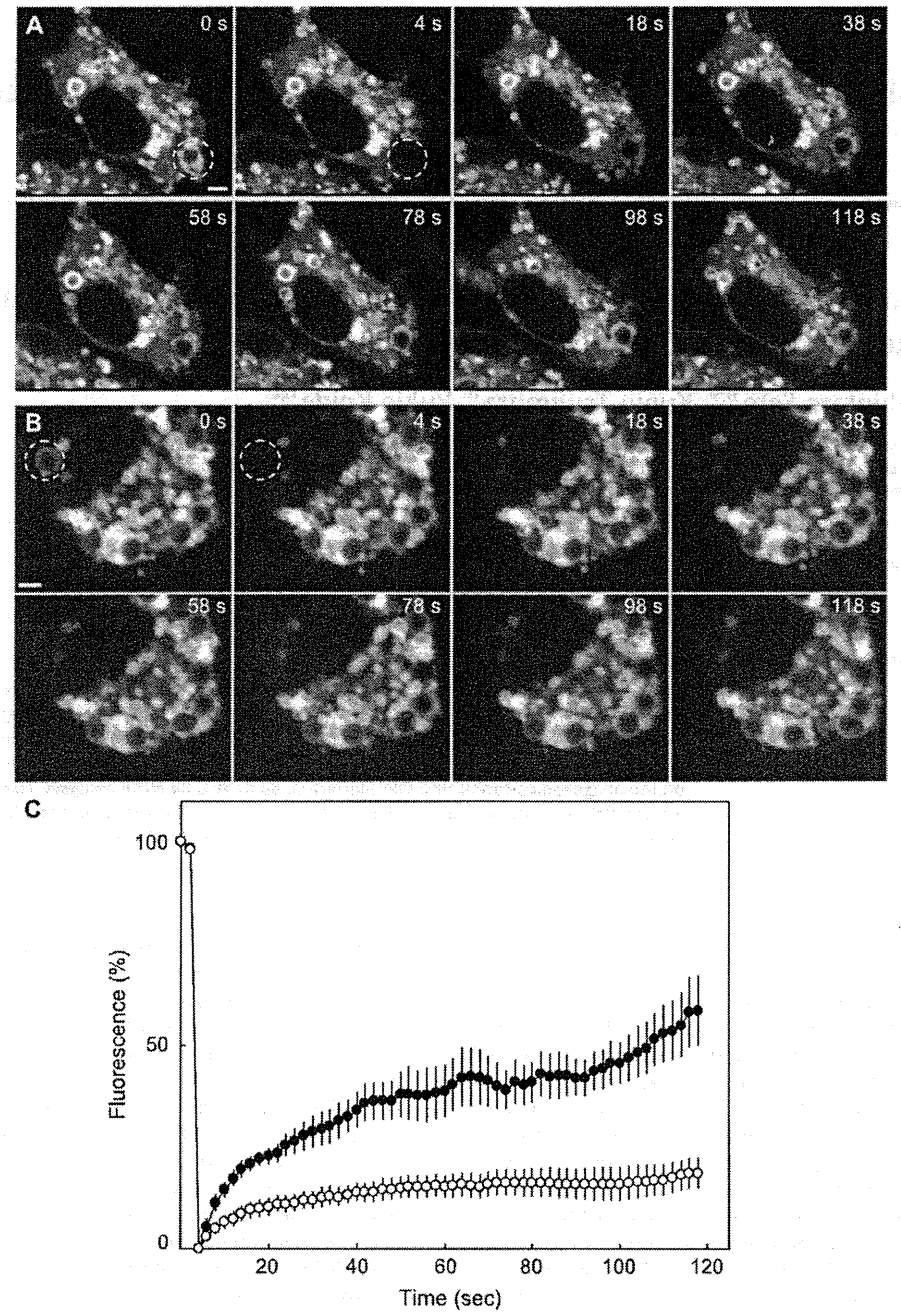

Fig. 1. FRAP analysis of EGFP-Rab7 on phagosomes. (A and B) Representative sequences of images from FRAP analysis of EGFP-Rab7 on phagosomes containing latex beads with (A) or without (B) IFN-γ stimulation. The regions marked by broken-line circles were photobleached for 4 s, and the recovery of fluorescence was monitored. (C) Temporal changes in fluorescence intensity on the bleached phagosomes. The relative intensity was defined as the ratio of fluorescence intensity at each time point to that at 0 s. The value zero was defined as the value obtained just after photobleaching. Closed and open circles indicate the relative intensities with ($n = 13$) or without ($n = 14$) IFN-γ stimulation, respectively. Data represent means and standard errors of means (SEM).

(FBS), 25 μg/ml penicillin G, and 25 μg/ml streptomycin at 37 °C under 5% CO_2. *M. bovis* BCG Tokyo transformed with a plasmid expressing DsRed [12] was grown to mid-logarithmic phase in 7H9 medium supplemented with 10% Middlebrook ADC (BD Biosciences), 0.5% glycerol and 0.05% Tween 80 containing 25 μg/ml kanamycin at 37 °C.

2.2. Plasmid constructs and transfection

Construction of the plasmid expressing enhanced green fluorescent protein (EGFP)-Rab7 has been previously described [10]. Human LAMP1 was amplified by PCR using cDNA derived from HeLa cells as a template, and the following primers: 5′-CTCGAGCCACCATGGCGGCCCCCGGCAGCGC-3′ and 5′-GGATCCCGATAGTCTGGTAGCCTGCGTGACTCCTC-3′. The PCR product corresponding to LAMP1 was inserted into pEGFP-N2 (Clontech). Transfection of cells was performed as described previously [10,11,13]. Briefly, 1×10^6 Raw264.7 macrophages were transfected with 10 μg of plasmid DNA using an MP-100 electroporator (Digital Bio Technology), according to the manufacturer's instructions. Transfected cells were grown in DMEM with 10% FBS for 24 h prior to the experiments. Transfected cells were incubated with murine IFN-γ

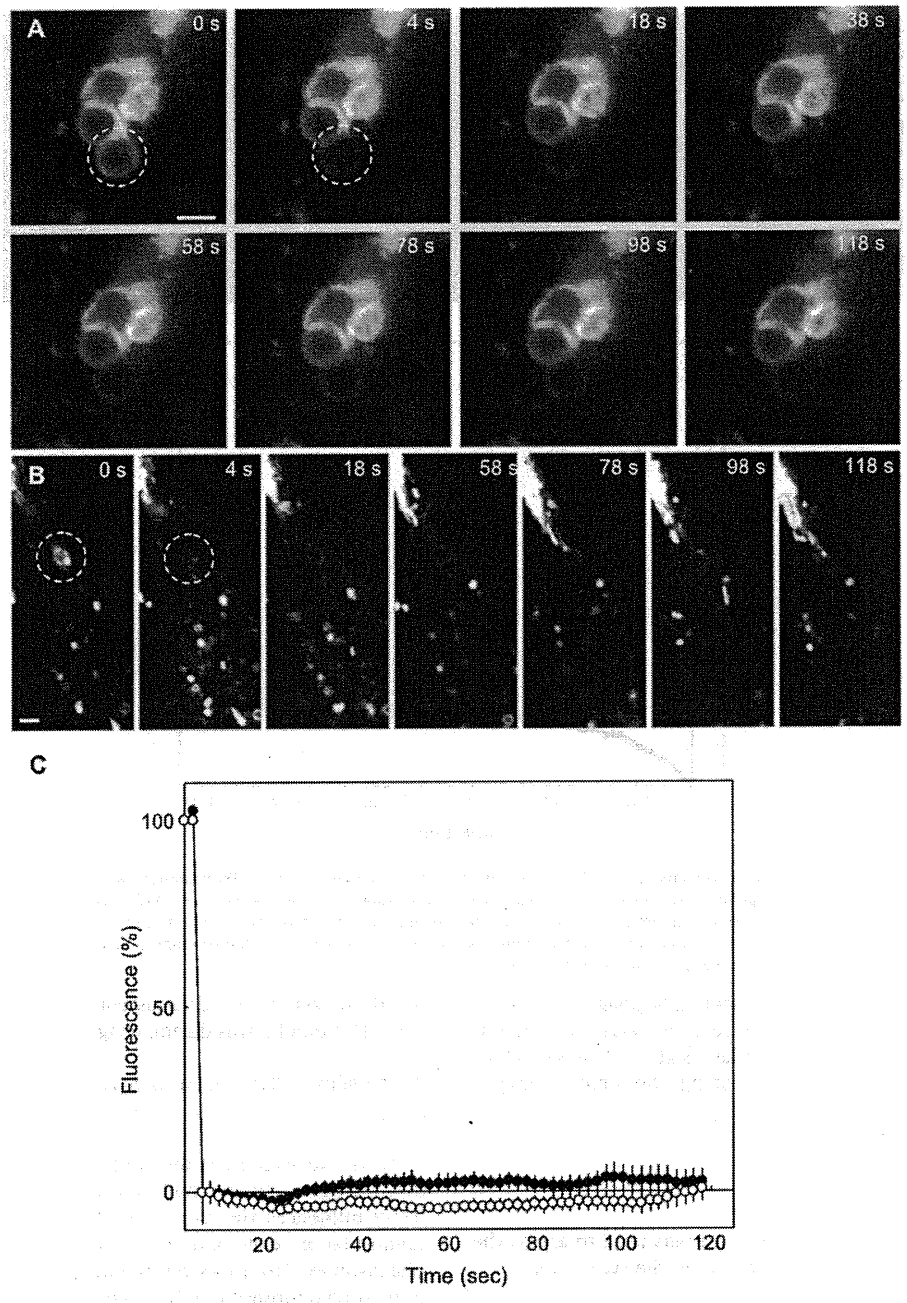

Fig. 2. FRAP analysis of LAMP1-EGFP on phagosomes. (A and B) Representative sequences of images from FRAP analysis of LAMP1-EGFP on phagosomes containing latex beads with (A) or without (B) IFN-γ stimulation. The regions marked by broken-line circles were photobleached for 4 s, and the recovery of fluorescence monitored. (C) Temporal changes in fluorescence intensity of bleached phagosomes. The relative intensity was defied as the ratio of intensity at each time point to that at 0 s. The value zero was defined as the value obtained just after photobleaching. Closed and open circles indicate the fluorescence intensities with (n = 14) or without (n = 13) IFN-γ stimulation, respectively. Data represent means and SEM.

(PeproTech, Inc.) at 10 ng/ml for 12 h before phagocytosis to activate the cells when required.

2.3. FRAP analysis

FRAP analysis was performed using an FV1000-D confocal microscope (Olympus) with a 60×/1.4 numerical aperture oil-immersion objective lens. Transfected cells (3×10^5 cells) grown on 35-mm glass dishes were allowed to phagocytose latex beads or *M. bovis* BCG expressing DsRed at 10–30 multiplicity of infection. Synchronous phagocytosis or infection was performed by centrifugation, washing with DMEM, and incubating with DMEM containing 10% FBS and 20 mM HEPES (pH 7.3) without phenol red. Temperature regulation of cells was carried out using an ONICS incubation system (Tokai Hit). The area of the phagosome surrounded by EGFP-Rab7 or LAMP1-EGFP was photobleached using a 410-nm laser at 15–20% power for 300 ms after pre-bleached images were acquired. Following photobleaching, the recovery of fluorescence was monitored at every 2 s using a 488-nm laser at 1–2% power for the phagosomes containing latex

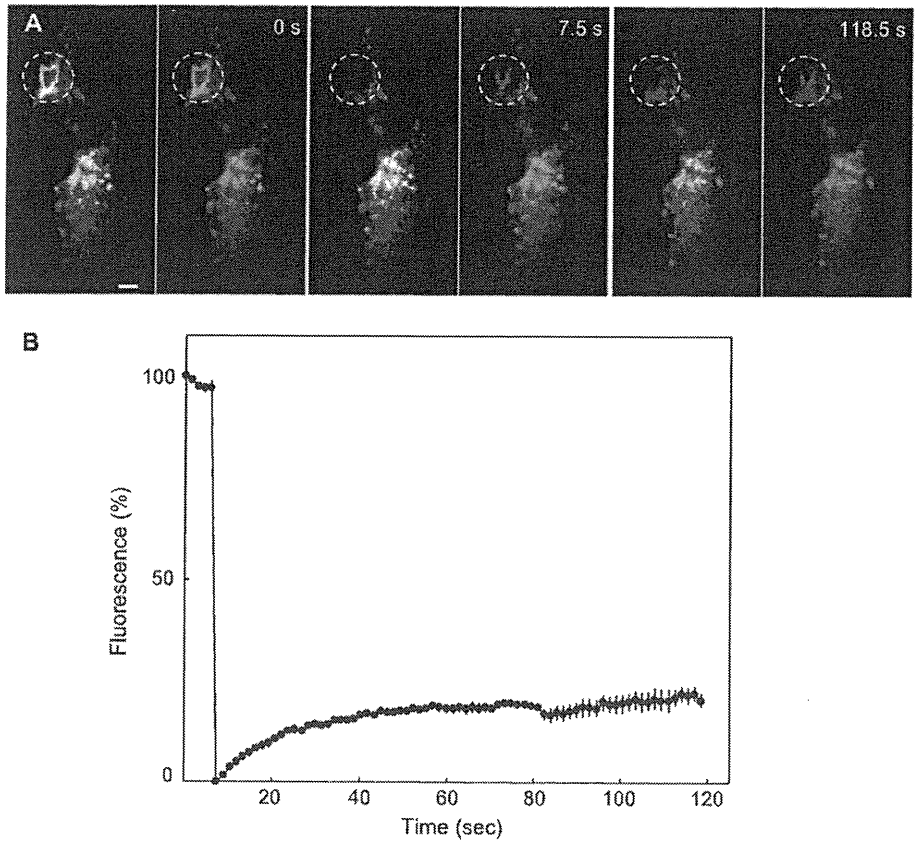

Fig. 3. FRAP analysis of EGFP-Rab7 on mycobacterial phagosomes. (A) A representative sequence of images from FRAP analysis of EGFP-Rab7 on a phagosome containing *M. bovis* BCG. Left and right panels at each time point show images of the macrophages expressing EGFP-Rab7 without and with images of infected *M. bovis* BCG expressing DsRed, respectively. The region marked by broken-line circles was photobleached for 6 s, and the recovery of fluorescence was monitored. (B) Temporal changes in fluorescence intensity of bleached phagosomes. The relative intensity was defined as the ratio of intensity at each time point to that at 0 s. The value zero was defined as the value obtained just after photobleaching. Data represent means and SEM ($n = 7$).

beads. For the measurement of fluorescence of phagosomes containing *M. bovis* BCG, the fluorescence recovery was measured at every 1.5 s using 488-nm and 543-nm lasers at 1–2% power. Fluorescence intensities were quantified using the ImageJ (http://rsb.info.nih.gp/ij/).

2.4. Statistics

The unpaired two-sided Student's *t*-test was used to assess the statistical significance of differences between the two groups.

3. Results and discussion

3.1. Mobility of Rab7 on phagosomes containing latex beads

To assess the mobility of Rab7, we conducted FRAP analysis on phagosomes containing latex beads in macrophages expressing EGFP-Rab7. Raw264.7 macrophages were transfected with a plasmid encoding EGFP-Rab7 and exposed to latex beads for 10 min, followed by phagosome maturation for 2 h. Phagosomes surrounded by EGFP-Rab7 were photobleached and the rate of recovery of fluorescence was monitored over time. A representative sequence of FRAP analysis is illustrated in Fig. 1A and Movie 1. After the phagosome with EGFP-Rab7 was photobleached (time: 4 s), fluorescence recovered rapidly. Quantitative analysis demonstrated that photobleached phagosomes recovered their fluorescence to 53% of the original level and the recovery half-time was 28 s (Fig. 1C). These results reflect the continuous conversion of Rab7 between GDP- and GTP-bound forms during phagosome maturation [14].

3.2. Mobility of Rab7 on the phagosomes in macrophages activated by IFN-γ

Next, we examined the mobility of Rab7 on phagosomes in macrophages activated by IFN-γ. Proteomic analysis revealed that IFN-γ influences the membrane trafficking on phagosomes containing latex beads and stimulates the accumulation of Rab7 to phagosomes [15]. However, the detailed kinetics of Rab7 localization on phagosomes in IFN-γ-activated macrophages has not been examined. Macrophages expressing EGFP-Rab7 were activated by IFN-γ for 12 h and allowed to phagocytose latex beads, with FRAP analysis performed 2 h after phagocytosis. As shown in Fig. 1B and Movie 2, after the phagosome was photobleached for 4 s, the fluorescence was very weak, even after 118 s. Quantitative analysis demonstrated that photobleached phagosomes recovered their fluorescence to 24% of the original level and the recovery half-time was 26 s (Fig. 1C). Previous reports demonstrated that the recovery of fluorescence was impaired in macrophages expressing the constitutive active form of Rab7 fused with GFP [16,17]. These results suggest that IFN-γ activates Rab7 on the phagosomes and consequently limits the conversion from its GTP- to GDP-bound form.

3.3. Mobility of LAMP1 on the phagosomes

To chase the mobility of LAMP1 on phagosomes, we conducted FRAP analysis on phagosomes in Raw264.7 macrophages expressing

LAMP1-EGFP. Macrophages transfected with LAMP1-EGFP were allowed to phagocytose latex beads; this was then followed by phagosome maturation for 2 h. Phagosomes surrounded by LAMP1-EGFP were photobleached and the recovery rate of fluorescence was monitored over time. As shown in Fig. 2A and Movie 3, the recovery of fluorescence was very weak, even after 118 s. Quantitative analysis revealed that the recovery rate of fluorescence was 19% of the original level and the recovery half-time for fluorescence was 42 s (Fig. 2C). FRAP analysis on phagosomes surrounded by LAMP1-EGFP in macrophages activated by IFN-γ revealed that addition of IFN-γ did not affect LAMP1 trafficking to the phagosomes (Fig. 2B and C and Mov. 4). These results suggest that LAMP1 is not directly sorted from the trans-Golgi network [18], but recruited by the fusion of lysosomal vesicles to the phagosomes.

3.4. Mobility of Rab7 on mycobacterial phagosomes

The localization of Rab7 on mycobacterial phagosomes has long been a controversial issue. Via et al. [19] first demonstrated that Rab7 does not localize to mycobacterial phagosomes, and this concept had been widely accepted [8,20]. However, Sun et al. [9] reported that Rab7 localizes to phagosomes containing *M. bovis* BCG. We also recently reported that Rab7 is transiently recruited to and subsequently released from phagosomes containing *M. tuberculosis* [10,11]. Besides localization, changes in the mobility of Rab7 on mycobacterial phagosomes have not been examined. In this study, we carried out FRAP analysis on Rab7-positive phagosomes containing *M. bovis* BCG (Fig. 3). Fig. 3A and Movie 5 illustrates a representative sequence from FRAP analysis of a mycobacterial phagosome. The mycobacterial phagosome surrounded by EGFP-Rab7 was photobleached at 6 s. The recovery of fluorescence by the mycobacterial phagosome was very weak 118.5 s after photobleaching, in contrast to that in phagosomes with latex beads (Fig. 1A). Quantitative analysis revealed that only 29% recovery was achieved and fluorescence recovery half-time was 25 s, suggesting that Rab7 is trapped in mycobacterial phagosomes. Previous reports demonstrated that RILP does not localize to mycobacterial phagosomes despite Rab7 localization [9,13]. The mobility of Rab7 is also restricted to the phagosomes containing *Salmonella* and *Burkholderia*, while RILP does not localize to these phagosomes despite Rab7 localization [16,17]. These results imply that mycobacteria may affect the activation state of Rab7 on phagosomes. Alternatively, mycobacterial phagosomes may acquire the ability to actively refuse the binding of Rab7, because the proportion of Rab7-positive mycobacterial phagosomes increases initially, then decreases 1 h after phagocytosis [10,11].

Acknowledgments

We thank Drs. Toshi Nagata and Masato Uchijima (Hamamatsu University School of Medicine, Hamamatsu, Japan) for their helpful discussions. We also thank Ms Yumiko Suzuki (Hamamatsu University School of Medicine) for her excellent assistance. This work was supported in part by Grants-in-Aid for Young Scientists (B), Scientific Research (B) and Scientific Research (C) from the Japan Society for the Promotion of Science; Scientific Research on Priority Areas from the Ministry of Education, Culture, Sports, Science and Technology of Japan; the Health and Labour Science Research Grants for Research into Emerging and Reemerging Infectious Diseases from the Ministry of Health, Labour and Welfare of Japan; and the United States-Japan Cooperative Medical Science Committee.

Appendix A. Supplementary data

Supplementary data associated with this article can be found, in the online version, at doi:10.1016/j.bbrc.2011.06.023.

References

[1] O.V. Vieira, R.J. Botelho, S. Grinstein, Phagosome maturation: aging gracefully, Biochem. J. 366 (2002) 689–704.
[2] O.V. Vieira, R.J. Botelho, L. Rameh, S.M. Brachmann, T. Matsuo, H.W. Davidson, A. Schreiber, J.M. Backer, L.C. Cantley, S. Grinstein, Distinct roles of class I and class III phosphatidylinositol 3-kinases in phagosome formation and maturation, J. Cell. Biol. 155 (2001) 19–25.
[3] O.V. Vieira, C. Bucci, R.E. Harrison, W.S. Trimble, L. Lanzetti, J. Gruenberg, A.D. Schreiber, P.D. Stahl, S. Grinstein, Modulation of Rab5 and Rab7 recruitment to phagosomes by phosphatidylinositol 3-kinase, Mol. Cell. Biol. 23 (2003) 2501–2514.
[4] R.E. Harrison, C. Bucci, O.V. Vieira, T.A. Schroer, S. Grinstein, Phagosomes fuse with late endosomes and/or lysosomes by extension of membrane protrusions along microtubules: role of Rab7 and RILP, Mol. Cell. Biol. 23 (2003) 6494–6506.
[5] E.L. Eskelinen, Y. Tanaka, P. Saftig, At the acidic edge: emerging functions for lysosomal membrane proteins, Trends Cell. Biol. 13 (2003) 137–145.
[6] K.K. Huynh, E.L. Eskelinen, C.C. Scott, A. Malevanets, P. Saftig, S. Grinstein, LAMP proteins are required for fusion of lysosomes with phagosomes, EMBO J. 26 (2007) 313–324.
[7] J. Rink, E. Ghigo, Y. Kalaidzidis, M. Zerial, Rab conversion as a mechanism of progression from early to late endosomes, Cell 122 (2005) 735–749.
[8] I. Vergne, J. Chua, S.B. Singh, V. Deretic, Cell biology of *Mycobacterium tuberculosis* phagosome, Annu. Rev. Cell. Dev. Biol. 20 (2004) 367–394.
[9] J. Sun, A.E. Deghmane, H. Soualhine, T. Hong, C. Bucci, A. Solodkin, Z. Hmama, *Mycobacterium bovis* BCG disrupts the interaction of Rab7 with RILP contributing to inhibition of phagosome maturation, J. Leukoc. Biol. 82 (2007) 1437–1445.
[10] S. Seto, S. Matsumoto, I. Ohta, K. Tsujimura, Y. Koide, Dissection of Rab7 localization on *Mycobacterium tuberculosis* phagosome, Biochem. Biophys. Res. Commun. 387 (2009) 272–277.
[11] S. Seto, K. Tsujimura, Y. Koide, Rab GTPases regulating phagosome maturation are differentially recruited to mycobacterial phagosomes, Traffic 12 (2011) 407–420.
[12] K. Aoki, S. Matsumoto, Y. Hirayama, T. Wada, Y. Ozeki, M. Niki, P. Domenech, K. Umemori, S. Yamamoto, A. Mineda, M. Matsumoto, K. Kobayashi, Extracellular mycobacterial DNA-binding protein 1 participates in mycobacterium-lung epithelial cell interaction through hyaluronic acid, J. Biol. Chem. 279 (2004) 39798–39806.
[13] S. Seto, S. Matsumoto, K. Tsujimura, Y. Koide, Differential recruitment of CD63 and Rab7-interacting-lysosomal-protein to phagosomes containing *Mycobacterium tuberculosis* in macrophages, Microbiol. Immunol. 54 (2010) 170–174.
[14] J.H. Brumell, M.A. Scidmore, Manipulation of rab GTPase function by intracellular bacterial pathogens, Microbiol. Mol. Biol. Rev. 71 (2007) 636–652.
[15] I. Jutras, M. Houde, N. Currier, J. Boulais, S. Duclos, S. LaBoissiere, E. Bonneil, P. Kearney, P. Thibault, E. Paramithiotis, P. Hugo, M. Desjardins, Modulation of the phagosome proteome by interferon-gamma, Mol. Cell Proteomics 7 (2008) 697–715.
[16] R.E. Harrison, J.H. Brumell, A. Khandani, C. Bucci, C.C. Scott, X. Jiang, B.B. Finlay, S. Grinstein, *Salmonella* impairs RILP recruitment to Rab7 during maturation of invasion vacuoles, Mol. Biol. Cell. 15 (2004) 3146–3154.
[17] K.K. Huynh, J.D. Plumb, G.P. Downey, M.A. Valvano, S. Grinstein, Inactivation of macrophage Rab7 by *Burkholderia cenocepacia*, J. Innate Immun. 2 (2010) 522–533.
[18] N.R. Cook, P.E. Row, H.W. Davidson, Lysosome associated membrane protein 1 (Lamp1) traffics directly from the TGN to early endosomes, Traffic 5 (2004) 685–699.
[19] L.E. Via, D. Deretic, R.J. Ulmer, N.S. Hibler, L.A. Huber, V. Deretic, Arrest of mycobacterial phagosome maturation is caused by a block in vesicle fusion between stages controlled by rab5 and rab7, J. Biol. Chem. 272 (1997) 13326–13331.
[20] V. Deretic, I. Vergne, J. Chua, S. Master, S.B. Singh, J.A. Fazio, G. Kyei, Endosomal membrane traffic: convergence point targeted by *Mycobacterium tuberculosis* and HIV, Cell. Microbiol. 6 (2004) 999–1009.

Hindawi Publishing Corporation
Clinical and Developmental Immunology
Volume 2011, Article ID 549281, 11 pages
doi:10.1155/2011/549281

Research Article

Novel Prophylactic Vaccine Using a Prime-Boost Method and Hemagglutinating Virus of Japan-Envelope against Tuberculosis

Masaji Okada,[1] Yoko Kita,[1] Toshihiro Nakajima,[2] Noriko Kanamaru,[1] Satomi Hashimoto,[1] Tetsuji Nagasawa,[2] Yasufumi Kaneda,[3] Shigeto Yoshida,[4] Yasuko Nishida,[1] Hitoshi Nakatani,[1] Kyoko Takao,[1] Chie Kishigami,[1] Shiho Nishimatsu,[1] Yuki Sekine,[1] Yoshikazu Inoue,[1] David N. McMurray,[5] and Mitsunori Sakatani[1]

[1] *Clinical Research Center, National Hospital Organization, Kinki-Chuo Chest Medical Center, 1180 Nagasone, Kitaku, Sakai, Osaka 591-8555, Japan*
[2] *Ikeda Laboratory, GenomIdea Inc., 1-8-31 Midorigaoka, Ikeda, Osaka 530-0043, Japan*
[3] *Division of Gene Therapy Science, Graduate School of Medicine, Osaka University, 2-2 Yamadaoka, Suita, Osaka 565-0871, Japan*
[4] *Department of Medical Zoology, Jichi Medical School, 3311-1 Yakushiji, Minamikawachi-machi, Tochigi 329-0498, Japan*
[5] *System Health Science Center, College of Medicine, Texas A&M University, College Station, TX 77843-1114, USA*

Correspondence should be addressed to Masaji Okada, okm@kch.hosp.go.jp

Received 8 September 2010; Revised 6 January 2011; Accepted 16 January 2011

Academic Editor: Nicholas West

Objective. *Mycobacterium tuberculosis* infection is a major global threat to human health. The only tuberculosis (TB) vaccine currently available is bacillus Calmette-Guérin (BCG), although it has no efficacy in adults. Therefore, the development of a novel vaccine against TB for adults is desired. *Method.* A novel TB vaccine expressing mycobacterial heat shock protein 65 (HSP65) and interleukin-12 (IL-12) delivered by the hemagglutinating virus of Japan- (HVJ)- envelope was evaluated against TB infection in mice. Bacterial load reductions and histopathological assessments were used to determine efficacy. *Results.* Vaccination by BCG prime with IgHSP65+murine IL-12/HVJ-envelope boost resulted in significant protective efficacy (>10,000-fold versus BCG alone) against TB infection in the lungs of mice. In addition to bacterial loads, significant protective efficacy was demonstrated by histopathological analysis of the lungs. Furthermore, the vaccine increased the number of T cells secreting IFN-γ. *Conclusion.* This vaccine showed extremely significant protection against TB in a mouse model, consistent with results from a similar paper on cynomolgus monkeys. The results suggest that further development of the vaccine for eventual testing in clinical trials may be warranted.

1. Introduction

Tuberculosis (TB) is a major global threat to human health, with about 2 million people dying every year from *Mycobacterium tuberculosis* infection. The only TB vaccine currently available is an attenuated strain of *Mycobacterium bovis*, bacillus Calmette-Guerin (BCG), although its efficacy against adult TB disease is unclear. Furthermore, multidrug-resistant TB (MDR-TB) and extremely drug-resistant TB (XDR-TB) are becoming big problems worldwide. For these reasons, a prophylactic and therapeutic vaccine against TB is sought. TB vaccines are classified into 4 main groups: (1) DNA vaccines, (2) recombinant BCG vaccines, (3) subunit vaccines, and (4) attenuated vaccines.

It is well established that protective immunity to *M. tuberculosis* depends on both $CD4^+$ and $CD8^+$ T cells [1–6]. DNA vaccines induce cellular immune responses, including the Th-1-type cellular immune response, and they prevent infections in animal models [7, 8]. In fact, several human clinical trials have recently been initiated to test the efficacy of DNA vaccines against emerging and re-emerging infectious diseases including hepatitis B [9], malaria [10–12], and HIV infections [13]. DNA vaccines have also shown their potential as TB vaccines in mouse

models [14–17]. However, in a guinea pig model, which is one of the most biologically relevant systems available for studying human pulmonary TB, DNA vaccines have not been proven more efficacious than BCG [18]. The efficacy of any experimental TB vaccine must be evaluated in human clinical trials, and a vaccine against TB is still anxiously awaited.

We have been developing a novel TB vaccine that is a DNA vaccine expressing mycobacterial heat shock protein 65 (HSP65) and interleukin-12 (IL-12), delivered by the hemagglutinating virus of Japan- (HVJ)- liposome or -envelope (HVJ-E) (HSP65 + IL-12/HVJ) [19–22]. The former vaccine was 100-fold more efficacious than BCG in a murine model on the basis of the elimination of *M. tuberculosis* [19]. In the present study, we demonstrated that the combination of BCG prime with HSP65 + IL-12/HVJ-E vaccine-boost was 10,000-fold more efficacious than BCG alone in a murine TB prophylactic model.

2. Materials and Methods

2.1. Bacteria. *M. tuberculosis* strains H37Rv and *M. bovis* BCG Tokyo, were kindly provided by Dr. I. Sugawara (JATA, Tokyo, Japan). *M. bovis* BCG Tokyo was maintained in synthetic Sauton's medium (Wako Chemicals, Osaka, Japan). For the mouse infection studies, a single colony of *M. tuberculosis* H37Rv was grown in Middlebrook 7H9 medium (DIFCO Laboratories, Detroit, MI; lot 137971 XA MD) supplemented with albumin-dextrose complex and grown at 37°C until approximately midlog phase. Aliquots were stored at −80°C and thawed 10 days before use. Each bacterium was grown to midlog phase in 7H9 medium.

2.2. Animals. Inbred and specific pathogen-free female BALB/c mice were purchased from Japan SLC (Shizuoka, Japan). Mice were maintained in isolator cages, manipulated in laminar flow hoods, and used between 8 and 10 weeks of age. All animal experiments were approved by the National Hospital Organization Kinki-chuo Chest Medical Center Animal Care and Use Committee. All vaccinations and experiments on isolated tissues were performed on anesthetized animals with sevoflurane. Infected animals were housed in individual microisolator cages in Biosafety Level (BL) 3 animal facility of the NHO Kinki-chuo Chest Medical Center.

2.3. Plasmid Construction. The *HSP65* gene was amplified from *M. tuberculosis* H37Rv genomic DNA, and cloned into pcDNA3.1 (+) (Invitrogen, San Diego, CA) to generate pcDNA-hsp65 (designated as HSP65 DNA) as described previously [19]. The *hsp65* gene was fused with mouse Igκ secretion signal sequence, and pcDNA-Ighsp65 (designated as IgHSP65 DNA) was generated. For construction of the mouse IL-12 (mIL-12) *p40* and *p35* single-chain genes, *mIL12p35* and *mIL12p40* genes were cloned from pcDNA-p40p35 [21], fused and cloned into pcDNA3.1 (+) to generate pcDNA-mIL12p40p35-F (designated as mIL-12 DNA).

2.4. HVJ-E Vaccination. HVJ-E was prepared as described previously (Figure 1) [19–23]. The HVJ-E complex was aliquoted and stored at −70°C until use. Groups of BALB/c mice were vaccinated 3 times at 3-week intervals with 100 μL of HVJ-E solution containing 50 μg of pcDNA-IgHSP65 and 50 μg of mIL12 DNA. These DNA vaccines were injected into both anterior muscles in the tibia. Mice were vaccinated using 1×10^6 colony-forming units (CFU) *M. bovis* BCG Tokyo by subcutaneous injection at 4 different sites (left-upper, right-upper, left-lower, and right-lower back). HVJ-E DNA vaccine containing pcDNA-IgHSP65 and -mIL12 DNA was designated as IgHSP65 + mIL-12/HVJ-E in this text.

2.5. Challenge Infection of Vaccinated Animals and Bacterial Load Determination. Mice were challenged by the intravenous route with 5×10^5 CFU of *M. tuberculosis* H37Rv 4 weeks after the third vaccination as described previously (Figure 2) [19, 24]. 0.2 mL of saline containing 5×10^5 CFU of H37Rv *Mycobacterium tuberculosis* were injected into tail vein of mice. At 5 and 10 weeks after *M. tuberculosis* H37Rv challenge, lungs, spleens, and livers were aseptically homogenized by using a homogenizer in saline, and serial dilutions of the organ homogenates were plated on 7H11 Middlebrook agar (Kyokuto. Tokyo, Japan). Plates were sealed and incubated at 37°C, and the number of colonies was counted 2 weeks later. Results were converted to $\log_{10}$ values. The $\log_{10}$ [mean ± standard deviation (S.D.)] values for CFU/organs/animals were calculated for each experimental group. Weight of lungs, liver, or spleen was measured by a balance (Sartorius Co. LP620S).

2.6. Histological Analysis. The lungs obtained from the mice were fixed with 10% buffered formalin and embedded in paraffin. Each block was sliced into 4-μm-thick sections and stained using hematoxylin and eosin. Semiquantitative morphometric analysis of pathological slides was performed by a method modified over that of Dascher et al. (2003) using a micrometer-attached microscope (Microphot-FXA, Nikon, Japan) [19, 25, 26]. The longer axis and minor axis of each granuloma in the field (×40 magnification) were measured and then multiplied and summed. Three random fields from each tissue section of mice were evaluated. The average score of the fields was designated as the granuloma index ($\times 10^{-2}$ mm^2). This method for the evaluation of granuloma area was significantly correlated with the granuloma area determined by a hematoxylin and eosin section scanning method.

2.7. ELISPOT Assay. The spleens were removed aseptically from vaccinated mice 3 weeks after the third vaccination. Antigen-specific IFN-γ-producing cells were determined by enzyme-linked immunosorbent spot (ELISPOT) as described previously [19]. Briefly, ELISPOT plates (MultiScreen IP Filtration plate MAIPS45; Millipore, Bedford, MA) were coated with antimouse IFN-γ MAb R4-6A2 (BD Biosciences Pharmingen. San Diego, CA). Spleen cells from vaccinated mice were suspended at 1×10^7 cells/mL (1×10^6 cells/well). The cells were placed into 6 antibody-coated wells, and rHSP65 protein (10 μg/mL) or PPD

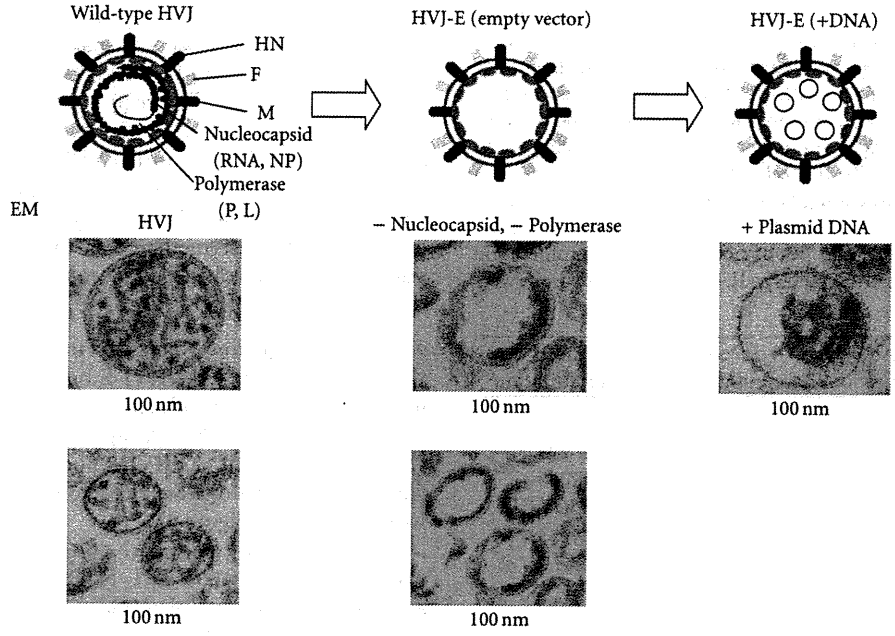

FIGURE 1: Hemagglutinating virus of Japan- (HVJ)- envelope vaccination: pcDNA3.1/HSP65DNA + IL-12DNA were incorporated into an HVJ-envelope empty vector (nonviral vector). Graphical representations of the HVJ-envelope empty vector in the presence or absence of DNA are shown. Electronic microscopy (EM) photographs of the HVJ-envelope empty vector are also shown.

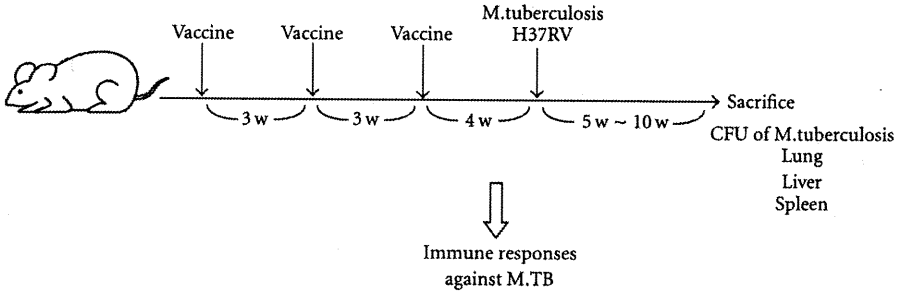

FIGURE 2: Groups of mice were vaccinated 3 times every 3 weeks using the prime-boost method and challenged intravenously with *M. tuberculosis* H37Rv as described in the Materials and Methods section. Five or 10 weeks after challenge with TB, protection was measured by enumerating bacterial loads (CFU) in the lungs, liver, and spleen of the vaccinated mice.

(10 μg/mL) was added to each well. After 20 h of incubation at 37°C, cells were removed by washing the plates, and the site of cytokine secretions was detected using biotinylated antimouse IFN-γ MAb XMG1.2 (BD Biosciences Pharmingen) and streptavidin-alkaline phosphatase conjugate (BD Biosciences Pharmingen). The enzyme reaction was developed with BCIP-NBT substrate (Vector Laboratories Inc., Burlingame, CA). Spot-forming cells (SFCs) were enumerated using the KS ELISPOT system (Carl Zeiss, Hallbergmoos, Germany).

2.8. Statistical Analysis. Dunnett's tests (multiple comparisons) were used to compare $\log_{10}$ values of CFUs between groups following challenge and used to compare T-cell responses between groups in the ELISPOT assay. A P-value of $< .05$ was considered significant.

3. Results and Discussion

3.1. Results

3.1.1. Prophylactic Efficacy Using Prime-Boost Method. The IgHSP65 + mIL-12/HVJ-E and BCG vaccines were administered using the prime-boost method as shown in Table 1.

At 5 and 10 weeks after intravenous challenge of *M. tuberculosis* H37Rv, the number of CFUs in the lungs, spleen, and liver were determined. Figure 3(a) shows the result of bacterial loads 5 weeks after challenge.

TABLE 1: BCG-HVJ-E/HSP65 DNA + IL-12 DNA Prime/Boost Experiment. Groups of mice were vaccinated 2 or 3 times with IgHSP65 + mIL-12/HVJ-E vaccine and/or BCG by using the prime-boost method. IgHSP65 + mIL-12/HVJ-E vaccine was injected intramuscularly, and BCG was injected subcutaneously. 4 weeks after the last immunization, *M. tuberculosis* H37Rv was challenged intravenously. 5 weeks and 10 weeks after TB challenge, protection was measured by enumerating bacterial loads (CFU) in the lungs, liver, and spleen from vaccinated mice. One week before the TB challenge, the immune responses of cytotoxic T cells, proliferation of T cells, and cytokines (IFN-γ, IL-2, IL-6) production were assayed.

Group	First immunization	Second immunization	Third immunization
1	—	—	—
2	—	—	BCG
3	HSP65 + IL-12/HVJ-E	HSP65 + IL-12/HVJ-E	HSP65 + IL-12/HVJ-E
4	BCG	HSP65 + IL-12/HVJ-E	HSP65 + IL-12/HVJ-E
5	HSP65 + IL-12/HVJ-E	HSP65 + IL-12/HVJ-E	BCG

13 mice per group.
3 mice for the *in vitro* assay prior to challenge (IFN-γ ELISPOT, etc.).
10 mice for the protection study (half of the mice were used for necropsy at 5 weeks after challenge and half at 10 weeks).

Vaccination by BCG prime + IgHSP65 + mIL-12/HVJ-E boost showed significant protective effects on the bacterial loads in the lungs as compared to BCG alone ($P < .01$). The prime-boost method using DNA and BCG vaccines showed extremely strong protective efficacy (>10,000-fold versus BCG alone) regardless of the order of administration (Figure 3(a)). Vaccination with BCG vaccine alone decreased TB CFUs in the lungs by 1 log unit as compared to nonvaccinated mice.

Vaccination with IgHSP65 + mIL-12/HVJ-E and BCG by the prime-boost method also showed significant protective efficacy on the bacterial loads in the liver as compared to BCG (>100-fold, $P < .05$; Figure 3(b)). The combination of 2 vaccines and administration by the prime-boost method also exerted a significant protective effect on the bacterial load in the spleen as compared to naive control group (10-fold higher, $P < .05$; Figure 3(c)).

Body weight of vaccinated mice was similar in all vaccinated groups. Tissue weights of spleens and livers in the prime-boost groups were lower than those of naive group (Figures 4 and 5).

We also confirmed the greater enhancement of protective effects in the BCG-DNA vaccine combination groups than those in the naive control group or BCG-alone group 10 weeks after challenge (data not shown). These results indicate that treatment using 2 vaccines by the prime-boost method was more effective than BCG alone.

3.1.2. Histological Analysis. In addition to the reduction of bacterial loads, the efficacies of each vaccine were assessed by histological analysis. The number and size of granulomatous lesions in the lungs were significantly lower and smaller, respectively, in the mice vaccinated by the BCG prime-DNA boost group than in the naive control mice and BCG control mice groups (Figure 6). Quantitative evaluation of the granulomatous lesions clearly showed that the BCG prime with IgHSP65 + mIL-12/HVJ-E boost significantly reduced the granuloma index in the lungs as compared to naive and BCG groups ($P < .05$; Figure 7). Thus, vaccination by the prime-boost method has the capability to reduce pulmonary lesions caused by *M. tuberculosis* infection.

3.1.3. Immunological Analysis. Furthermore, BCG prime with IgHSP65 + mIL-12/HVJ-E boost augmented the proliferation and IFN-γ production of HSP65 antigen-specific T cells in the K-S ELISPOT Assay. The efficacy of BCG prime with IgHSP65 + mIL-12/HVJ-E boost was higher compared with BCG Tokyo alone or IgHSP65 + mIL-12/HVJ-E prime with BCG boost (Figure 8).

These data indicate that the protective efficacies of BCG prime with IgHSP65 + mIL-12/HVJ-E boost are strongly associated with the number and activity of IFN-γ-secreting and HSP65-specific T cells. Taken together, combinational vaccination with BCG and IgHSP65 + mIL-12/HVJ-E by the prime-boost method is capable of augmenting T-cell activation. In addition, increase of IFN-γ-secreting cells is involved in the reduction of bacterial burden and lesions in the lungs. The efficacies of the prime-boost method are greater than those achieved by vaccination with BCG alone.

3.2. Discussion. In this study, we evaluated the protective efficacy of IgHSP65 + mIL-12/HVJ-E vaccine, using the prime-boost method. One of the significant findings was that the combination of IgHSP65 + mIL-12/HVJ-E and BCG led to a remarkably high degree of protection against intravenous challenge infection with virulent *M. tuberculosis*; bacterial numbers exponentially declined in 3 organs, especially in the lungs (10,000-fold lower than that of mice vaccinated with BCG alone; Figure 3(a)).

The pathological parameters of protection included reductions in the mean lung granulomatous lesion score in our study. The protective efficacies of BCG with IgHSP65 + mIL-12/HVJ-E administered by the prime-boost method were indicated on the basis of histopathological methods as well as bacterial loads. Histopathological analysis showed that mice vaccinated with BCG prime with IgHSP65 + mIL-12/HVJ-E boost had fewer and smaller lesions in the lungs and significantly less lung granuloma than naive mice and mice treated with BCG alone. These results suggest that severe toxicities (Koch phenomenon) were suppressed by the combination of two kinds of vaccines.

The data in the present study also show that the protective efficacy of BCG prime with IgHSP65 + mIL-12/HVJ-E boost is strongly associated with the emergence of IFN-γ-secreting T cells upon stimulation with HSP65. In the previous study, we demonstrated that *in vivo* function of CD8-positive T cells as well as CD4-positive T cells is involved in prophylactic efficacy of the IgHSP65 + mIL-12/HVJ-E in mice [22].

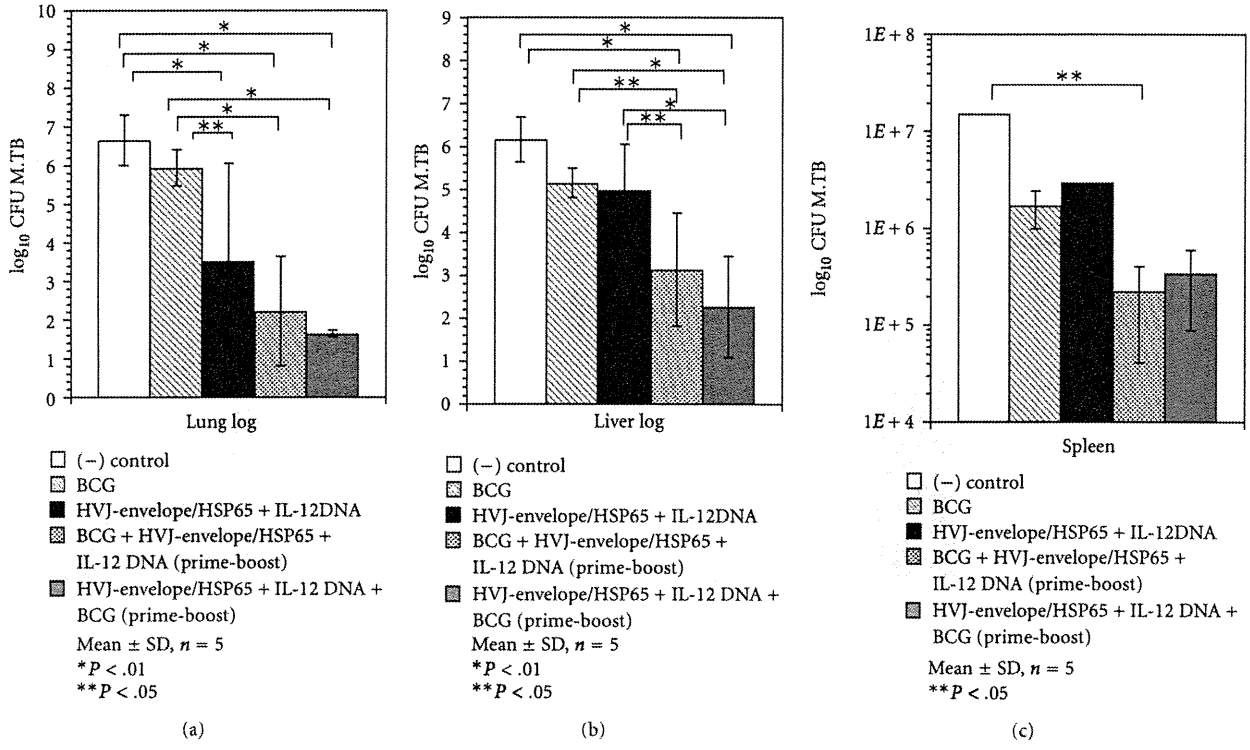

FIGURE 3: (a) Mouse protection studies using the prime-boost method. Groups of mice vaccinated with HVJ-envelope (HVJ-E) DNA and/or BCG were challenged by intravenous injection with *M. tuberculosis* H37Rv. Five weeks after challenge, protection was measured by enumerating the bacterial loads (CFU) in the lungs. Results are expressed as the mean $\log_{10}$ ± S.D. of CFU. The statistical significance of differences between individual groups in the CFU number was determined by Dunnett test ($n = 5$); $^*P < .01$ and $^{**}P < .05$; the statistical significance of differences ($P < .01$) of the G1 (naive) group compared to the G3 group (DNA/DNA/DNA), G4 group (BCG/DNA/DNA), or the G5 group (DNA/DNA/BCG). The statistical significance of differences ($^{**}P < .05$) of the G2 group (BCG-alone group) compared to the G3 group (DNA/DNA/DNA), that of differences ($P < .01$) of the G2 group compared to the G4 group (BCG/DNA/DNA), or the G5 group (DNA/DNA/BCG). (b) Mouse protection studies using the prime-boost method. Groups of mice vaccinated with HVJ-E DNA and/or BCG were challenged by intravenous injection with *M. tuberculosis* H37Rv. Five weeks after challenge, protection was measured by enumerating the bacterial loads (CFU) in the liver. Results are expressed as the mean $\log_{10}$ ± S.D. of CFU. The statistical significance of differences between individual groups in the CFU number was determined by Dunnett test ($n = 5$), $^*P < .01$; the statistical significance of differences ($P < .01$) of the G1 (naive) group compared to the G4 group (BCG/DNA/DNA), or the G5 group (DNA/DNA/BCG). The statistical significance of differences ($P < .05$) of the G2 group (BCG-alone group) compared to the G4 group (BCG/DNA/DNA). The statistical significance of differences($P < .01$) of the G2 group compared to the G5 group (DNA/DNA/BCG). The statistical significance of differences ($P < .05$) of the G3 group (DNA/DNA/DNA) compared to G4 (BCG/DNA/DNA). That of differences ($P < .01$) of the G3 group compared to the G5 group. (c) Mouse protection studies using the prime-boost method. Groups of mice vaccinated with HVJ-E DNA and/or BCG were challenged by intravenous injection with *M. tuberculosis* H37Rv. Five weeks after challenge, protection was measured by enumerating the bacterial loads (CFU) in the spleen. Results are expressed as the mean $\log_{10}$ ± S.D. of CFU. The statistical significance of differences between individual groups in the number of CFU was determined by Dunnett test ($n = 5$); $^{**}P < .05$; the statistical significance of differences ($P < .05$) of the G1 (naive) group compared to the G4 group (BCG/DNA/DNA).

In this study, we used the murine model of TB, which may not reflect the pathologic status of human TB. As to the difference of the infection route, our previous results in a guinea pig model used in a collaborative study with Dr. D. McMurray (Texas A&M University) showed that vaccination with HSP65 + guinea pig IL-12/HVJ resulted in better protection against pulmonary pathology caused by aerosol challenge with *M. tuberculosis* than BCG vaccination (data not shown).

In addition, we have recently confirmed that the prime-boost method was also effective in a cynomolgus monkey model [20–22]. We evaluated our HSP65 + human IL-12/HVJ (HSP65 + hIL-12/HVJ) in the monkey model infected by an intratracheal instillation (aerogenic route), which is currently the best animal model of human TB. Vaccination with HSP65 + hIL-12/HVJ resulted in better protective efficacy than that with BCG alone on the basis of the erythrocyte sedimentation rate test, chest X-ray findings, and immune responses. In addition, vaccination with HSP65 + hIL-12/HVJ resulted in increased survival for over a year. This was the first report of successful DNA vaccination against M. tuberculosis in a monkey model [21].

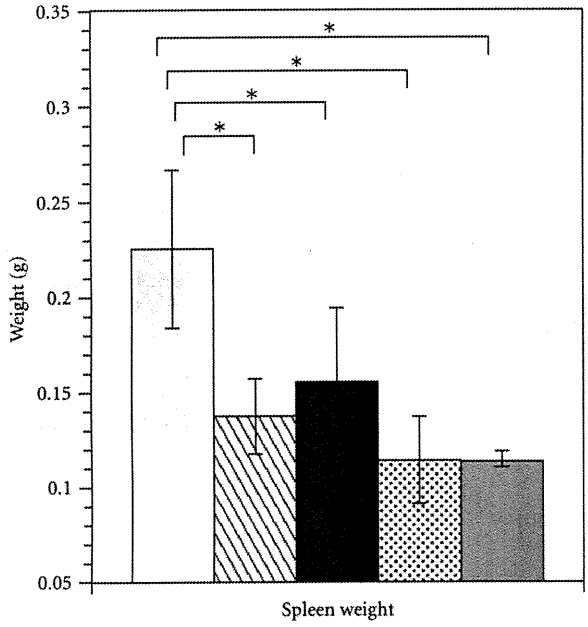

FIGURE 4: Tissue weight in mouse protection studies using the prime-boost method. Groups of mice vaccinated with HVJ-E DNA and/or BCG were challenged by intravenous injection with *M. tuberculosis* H37Rv. Five weeks after challenge, spleen weight was measured. Results are expressed as the mean ± S.D. in grams (g). The statistical significance of differences between individual groups in the weight was determined by Dunnett test ($n = 5$), $^*P \leq .01$; the statistical significance of differences ($P < .01$) of the G1 (naive) group compared to the G2 group (BCG-alone group), G3 group (DNA/DNA/DNA), G4 group (BCG/DNA/DNA), or G5 group (DNA/DNA/BCG).

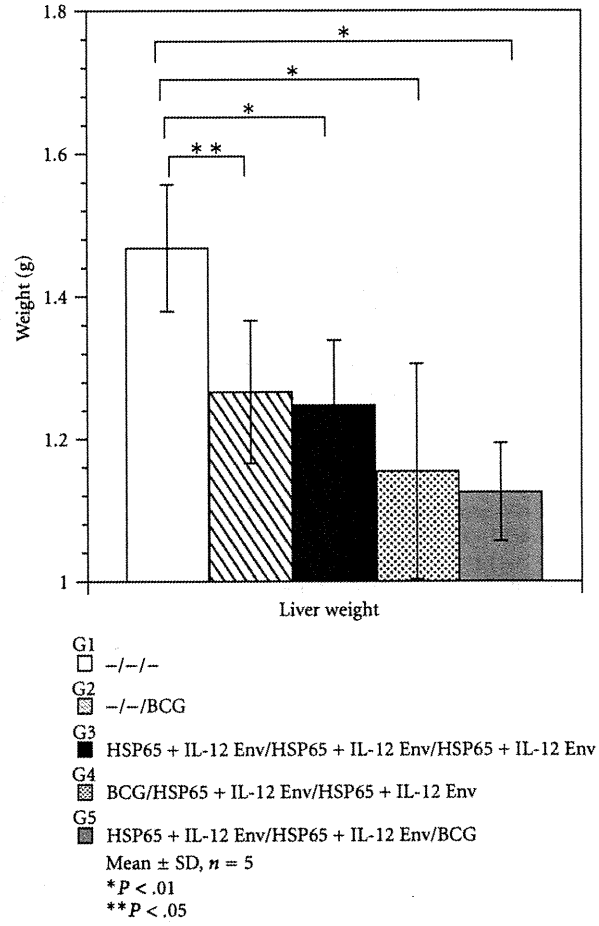

FIGURE 5: Tissue weight in mouse protection studies using the prime-boost method. Groups of mice vaccinated with HVJ-E DNA and/or BCG were challenged by intravenous injection with *M. tuberculosis* H37Rv. Five weeks after challenge, liver weight was measured. Results are expressed as the mean ± S.D. in grams (g). The statistical significance of differences between individual groups in the weight was determined by Dunnett test ($n = 5$), $^*P < .01$; the statistical significance of differences ($P \leq .01$) of the G1 (naive) group compared to the G3 group (DNA/DNA/DNA), G4 group (BCG/DNA/DNA), or G5 group (DNA/DNA/BCG). $^{**}P < .05$; that of differences ($P < .05$) of the G1 group compared to the G2 group (BCG alone group).

Most importantly, protective efficacy was augmented when BCG and HSP65 + hIL-12/HVJ were administered by the prime-boost method. Survival rates of BCG alone, saline control, HSP65 + hIL-12/HVJ-prime with BCG-boost, and BCG-prime with HSP65 + hIL-12/HVJ-boost groups were 33%(2/6), 50%(3/6), 50%(2/4), and 100%(4/4) at 12 months after the infection (aerogenic route), respectively [21]. We also evaluated immune responses in the monkey model of TB. Antigen-specific IFN-γ-production and proliferation of peripheral blood lymphocyte (PBL) were enhanced by the vaccination using the prime-boost method.

We also demonstrated efficacies in the monkey model when the boost was performed after a long-term period (4 months) from the prime. The prolongation of the survival was observed in the BCG-prime and HSP65 + IL-12/HVJ-booster group [27]. Improvement of ESR, increase of the body weight and augmentation of IFN-γ production, and proliferation of PBL were also observed in the BCG-prime and HSP65 + IL-12/HVJ-booster group.

Taken together, these results clearly demonstrated that BCG-prime with HSP65 + hIL-12/HVJ-boost could provide extremely strong protective efficacy against M. tuberculosis in a cynomolgus monkey model (intratracheal infection route), which is currently the best animal model of human TB [21].

The prime-boost method was reported in a study of the MVA85A vaccine, which is a modified vaccinia virus Ankara (MVA) strain expressing antigen 85A. In phase I studies in humans, this vaccine has induced high immune responses in previously BCG-vaccinated individuals [28].

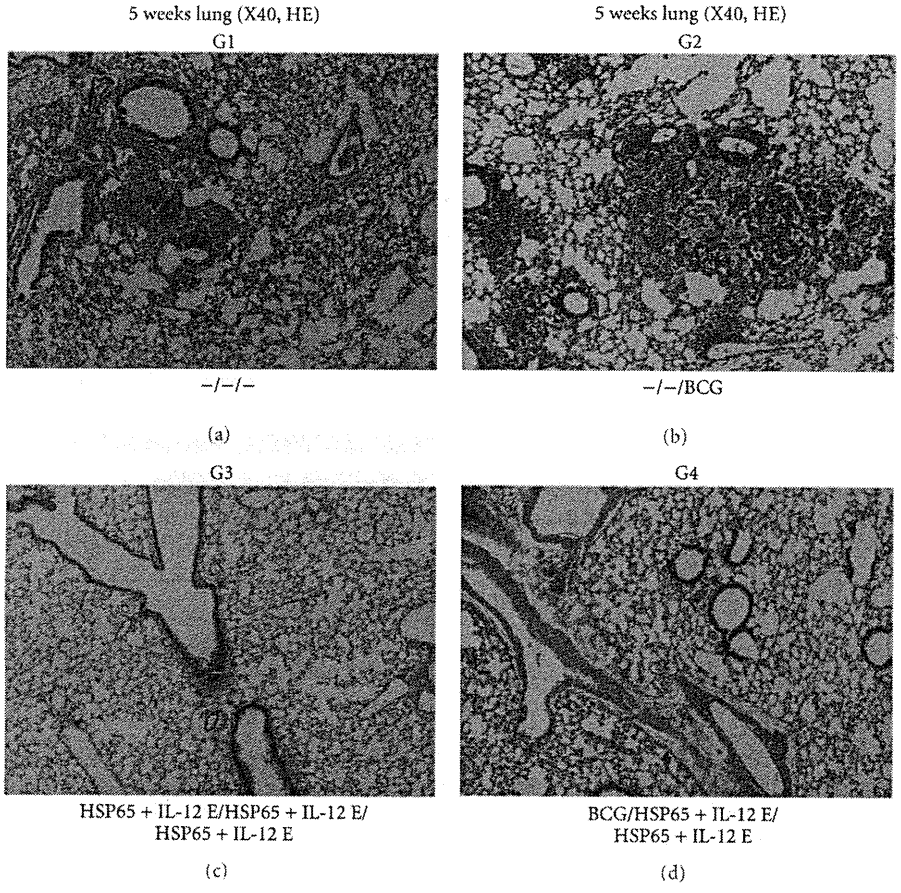

FIGURE 6: Histopathological analysis of vaccinated mice 5 weeks after *M. tuberculosis* challenge. Representative photomicrographs of lung tissue sections harvested from the G1 naive control group, G2 (BCG alone) group, G3 group (DNA/DNA/DNA), and G4 group (BCG/DNA/DNA) are shown (5 weeks after *M. tuberculosis* challenge, hematoxylin and eosin staining, × 4 objective). There was much infiltration of mononuclear cells and extensive parenchymal destruction by large, poorly demarcated granuloma in the lungs from the G1 (naive control) group and G2 (BCG alone) group. In the G3 (DNA/DNA/DNA) group and G4 (BCG/DNA/DNA) group, there was less inflammation, and only a few granulomas were observed.

Boosting BCG vaccination with MVA85A downregulates the immunoregulatory cytokine TGF-β1 [29]. Aeras-402 DNA (DNA that expressed 85A, 85B, and TB10.4) vaccine using adenovirus vector is intended for use as a boosting vaccine in BCG-primed individuals [30]. Several vaccines have been used with a prime-boost strategy to complement immune responses [31].

DNA vaccines are a relatively new approach to induce immunities for the protection of infectious diseases [14, 19, 22, 32–34]. Prophylactic and therapeutic DNA vaccines were established by using several kinds of vectors such as HVJ-liposome, HVJ-E, adenovirus vector, adenoassociated virus vector, and lentivirus vector [19–22, 35, 36]. In order to explore the preclinical use of a tuberculosis DNA vaccine combination of *IL-12* DNA with *hsp65* DNA, we chose the HVJ-based delivery system (HVJ-liposome and HVJ-E). These systems have high transfection efficiency and are available for repeated *in vivo* gene transfection without reduction of gene transfer efficiency or apparent toxicity. These characters of HVJ-liposomes support the feasibility of its clinical application not only for cancer gene therapy but also for DNA vaccinations. In a recent study, highly efficient gene expression in muscle cells was observed for several weeks when pcDNA3 plasmid containing the human tumor antigen genes, *MAGE-1* and *MAGE-3*, were encapsulated in HVJ-liposomes and injected intramuscularly in mice [37]. Effective induction of $CD4^+$ T-cell responses by a hepatitis B core particle-based HIV vaccine was achieved by subcutaneous administration of HVJ-liposomes in mice [38]. HVJ-liposomes were also very effective as a mucosal vaccine against HIV infection [39]. Thus, it is likely that HVJ proteins may be responsible for the induction of a robust immune response. No side effects were observed when repetitive injections of HVJ-liposomes were performed in mice, rats, or monkeys. We have previously developed an HVJ-E using inactivated Sendai virus, as a nonviral vector for drug delivery [40–42]. It can be used for efficient delivery of DNAs, siRNAs, proteins, and anticancer drugs into cells

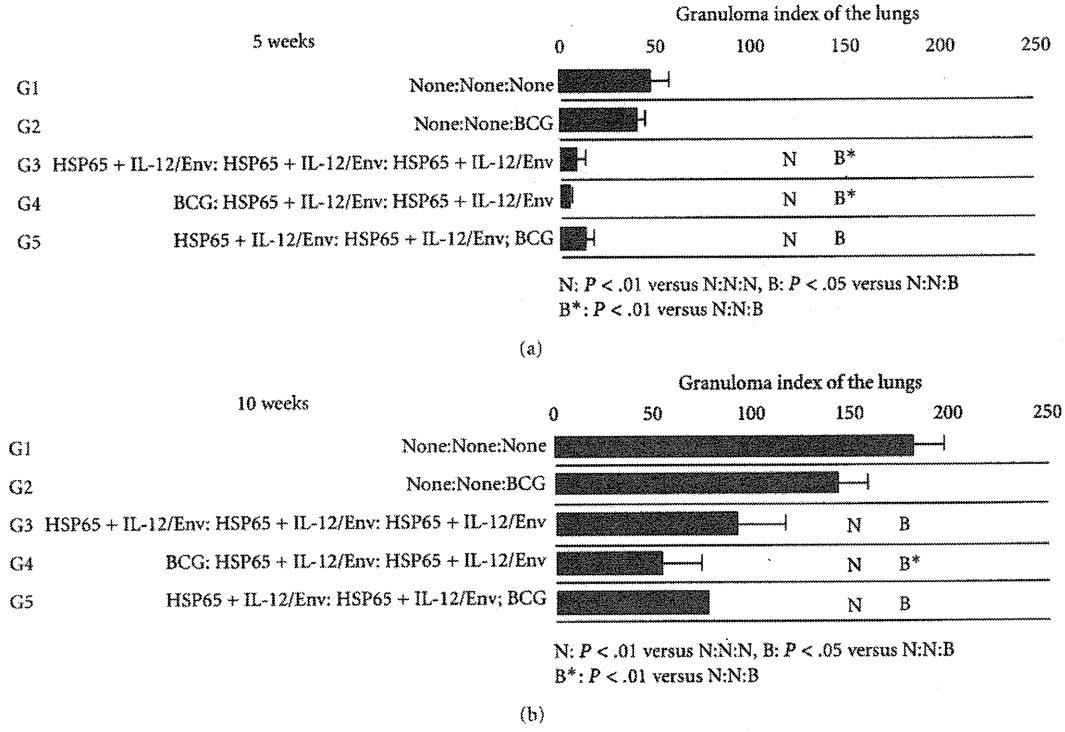

FIGURE 7: Granuloma index of the G1, G2, G3, G4, and G5 (DNA/DNA/BCG) groups in the lungs 5 weeks and 10 weeks after *M. tuberculosis* challenge. Results are expressed as the mean ± S.D. of triplicates of 5 mice per group. The statistical significance of differences between the groups was determined by Dunnett test, $P < .01$ as compared with the naive (N) group or the BCG alone (B) group. $P < .05$ as compared with the BCG alone (B*) group. The statistical significance of differences ($P < .05$) of granuloma index of 5 weeks G3 group compared to the G4 group.

both *in vitro* and *in vivo* [40, 43, 44]. Therefore, HVJ-E was used as an efficient and safe vector for DNA vaccine against TB in the present study.

Mycobacterial heat shock protein 65 (HSP65) is a potential target for protective immunity and has been studied extensively [19]. Several studies have reported that *hsp65* DNA vaccines can strongly induce protective immune responses in mice against virulent *M. tuberculosis* infections [20–22]. Protection is attributed to the establishment of a cellular immune response dominated by HSP65-specific T cells which produce IFN-γ and are cytotoxic towards infected cells. Furthermore, Lowrie and colleagues have reported that this vaccine reduces bacterial loads in mice infected with *M. tuberculosis* when given therapeutically after infection [32].

One of the major roles of IL-12 is the induction of IFN-γ-mediated immune responses to microbial pathogens. Cooper and colleagues have demonstrated the importance of IL-12 in generation of the protective response to tuberculosis [45]. Coadministration of the *IL-12* gene, which induces an IFN-γ-mediated immune response to microbial pathogens, with various tuberculosis DNA vaccines including *hsp65* DNA [46], and 35 K MW DNA [47], may boost the efficacy of these DNA vaccines to the levels achieved with BCG in the mouse model, although an inhibitory effect rather than a synergistic effect on immunotherapy was observed in mice coadministered *hsp65* DNA vaccine plus the *IL-12* gene [32].

In conclusion, we have shown efficacy of a novel HVJ-E DNA vaccine encapsulating HSP65 DNA with IL-12 DNA in the mouse model of TB. These results suggest that HSP65 + IL-12/HVJ could be a promising candidate for a new tuberculosis vaccine superior to BCG. To this aim, protective efficacy and immune responses were further studied in nonhuman primates before proceeding to human clinical trials.

In Japan and other countries, BCG is inoculated into human infants up to 6 months after birth. Therefore, BCG prime in infants and HSP65 + hIL-12/HVJ boost in adults (including junior high school students, high school students, and the elderly) may be required for significant improvement of clinical protective efficacy against TB. Thus, our results with the HSP65 + hIL-12/HVJ vaccine in a murine prophylactic model and cynomolgus monkey prophylactic model provide a significant rationale for moving this vaccine into clinical trials. Indeed, multiple animal models are available to accumulate essential data on the HVJ-E DNA vaccine in anticipation of a phase I clinical trial.

4. Conclusions

Vaccination by BCG prime with a novel vaccine (IgHSP65 + mIL-12/HVJ-E) boost resulted in significant protective efficacy (10,000-fold greater than BCG alone) against TB

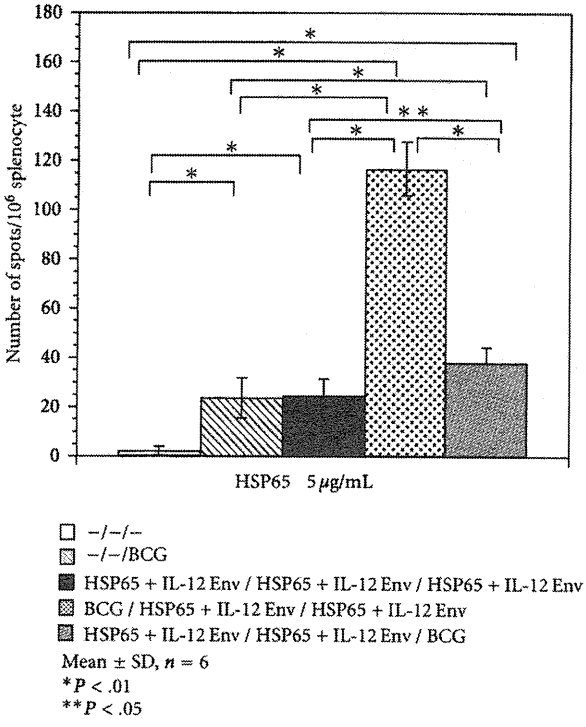

FIGURE 8: ELISPOT assay for IFN-γ antigen-specific responses in the spleens of vaccinated mice following stimulation with rHSP65 protein. Spleen cell cultures were stimulated with rHSP65 protein for 20 h. The numbers of IFN-γ-secreting cells specific for rHSP65 protein per million cells were determined individually by ELISPOT assay. Results are expressed as the mean ± S.D. of 6 wells of 3 mice per group. The statistical significance of differences between individual groups in the number of IFN-γ-secreting cells was determined by Dunnett test. The statistical significance of differences ($P < .01$) of the G1 (naive) group compared to the G2 (BCG alone group), G3 (DNA/DNA/DNA), G4 (BCG/DNA/DNA), or G5 (DNA/DNA/BCG). The statistical significance of the G2 group difference ($P < .01$) compared to the G4 or the G5. The statistical significance of the G3 group differences ($P < .01$) compared to the G4. $P < .01$; the G4 group compared to the G5. The statistical significance of the G3 group differences ($P < .05$) compared to the G5.

infection in the lungs of mice. In addition to bacterial loads, significant protective immunity was demonstrated by histopathological analysis of the lungs. This vaccine showed extremely significant protection against TB, suggesting that further development for eventual testing in clinical trials may be warranted.

Acknowledgments

This paper was supported by Health and Labor Science Research Grants from MHLW, international collaborative study Grants from the Human Science foundation, and Grant-in-Aid for Scientific Research (B) from the Ministry of Education, Culture, Sports, Science, and Technology (Japan), Research on Publicly Essential Drugs and Medical Devices from Japan Health Sciences Foundation, and a Grant from the Osaka Tuberculosis Foundation.

References

[1] J. L. Flynn and J. Chan, "Immunology of tuberculosis," *Annual Review of Immunology*, vol. 19, pp. 93–129, 2001.

[2] J. Hess, U. Schaible, B. Raupach, and S. H. E. Kaufmann, "Exploiting the immune system: toward new vaccines against intracellular bacteria," *Advances in Immunology*, vol. 75, pp. 1–88, 2000.

[3] A. Geluk, K. E. Van Meijgaarden, K. L. M. C. Franken et al., "Identification of major epitopes of *Mycobacterium tuberculosis* AG85B that are recognized by HLA-A*0201-restricted $CD8^+$ T cells in HLA-transgenic mice and humans," *Journal of Immunology*, vol. 165, no. 11, pp. 6463–6471, 2000.

[4] A. Lalvani, R. Brookes, R. J. Wilkinson et al., "Human cytolytic and interferon γ-secreting CD8+ T lymphocytes specific for *Mycobacterium tuberculosis*," *Proceedings of the National Academy of Sciences of the United States of America*, vol. 95, no. 1, pp. 270–275, 1998.

[5] P. Wong and E. G. Pamer, "CD8 T cell responses to infectious pathogens," *Annual Review of Immunology*, vol. 21, pp. 29–70, 2003.

[6] H. McShane, S. Behboudi, N. Goonetilleke, R. Brookes, and A. V. S. Hill, "Protective immunity against *Mycobacterium tuberculosis* induced by dendritic cells pulsed with both CD8(+)- and CD4(+)-T-cell epitopes from antigen 85A," *Infection and Immunity*, vol. 70, no. 3, pp. 1623–1626, 2002.

[7] I. K. Srivastava and M. A. Liu, "Gene vaccines," *Annals of Internal Medicine*, vol. 138, no. 7, pp. 550–148, 2003.

[8] M. Okada and T. Kishimoto, "The potential application and limitation of cytokine/growth factor manipulation in cancer therapy," in *Cell proliferation in Cancer: Regulatory Mechanisms of Neoplastic Cell Growth*, L. Pusztai, C. Lewis, and E. Yap, Eds., pp. 218–244, Oxford University Press, New York, NY, USA, 1996.

[9] M. J. Roy, M. S. Wu, L. J. Barr et al., "Induction of antigen-specific $CD8^+$ T cells, T helper cells, and protective levels of antibody in humans by particle-mediated administration of a hepatitis B virus DNA vaccine," *Vaccine*, vol. 19, no. 7-8, pp. 764–778, 2000.

[10] T. P. Le, K. M. Coonan, R. C. Hedstrom et al., "Safety, tolerability and humoral immune responses after intramuscular administration of a malaria DNA vaccine to healthy adult volunteers," *Vaccine*, vol. 18, no. 18, pp. 1893–1901, 2000.

[11] A. C. Moore and A. V. S. Hill, "Progress in DNA-based heterologous prime-boost immunization strategies for malaria," *Immunological Reviews*, vol. 199, pp. 126–143, 2004.

[12] S. Yoshida, S. I. Kashiwamura, Y. Hosoya et al., "Direct immunization of malaria DNA vaccine into the liver by gene gun protects against lethal challenge of Plasmodium berghei sporozoite," *Biochemical and Biophysical Research Communications*, vol. 271, no. 1, pp. 107–115, 2000.

[13] J. D. Boyer, M. A. Chattergoon, K. E. Ugen et al., "Enhancement of cellular immune response in HIV-1 seropositive individuals: a DNA-based trial," *Clinical Immunology*, vol. 90, no. 1, pp. 100–107, 1999.

[14] K. Huygen, "DNA vaccines: application to tuberculosis," *International Journal of Tuberculosis and Lung Disease*, vol. 2, no. 12, pp. 971–978, 1998.

[15] D. B. Lowrie, "DNA vaccines against tuberculosis," *Current Opinion in Molecular Therapeutics*, vol. 1, no. 1, pp. 30–33, 1999.

[16] I. M. Orme, "The search for new vaccines against tuberculosis," *Journal of Leukocyte Biology*, vol. 70, no. 1, pp. 1–10, 2001.

[17] T. M. Doherty and P. Andersen, "Tuberculosis vaccine development," *Current Opinion in Pulmonary Medicine*, vol. 8, no. 3, pp. 183–187, 2002.

[18] D. M. McMurray, "Guinea pig model of tuberculosis," in *Tuberculosis: Pathogenesis, Protection, and Control*, pp. 113–134, ASM Press, Washington, DC, USA, 1994.

[19] S. Yoshida, T. Tanaka, Y. Kita et al., "DNA vaccine using hemagglutinating virus of Japan-liposome encapsulating combination encoding mycobacterial heat shock protein 65 and interleukin-12 confers protection against *Mycobacterium tuberculosis* by T cell activation," *Vaccine*, vol. 24, no. 8, pp. 1191–1204, 2006.

[20] Y. Kita, T. Tanaka, S. Yoshida et al., "Novel recombinant BCG and DNA-vaccination against tuberculosis in a cynomolgus monkey model," *Vaccine*, vol. 23, no. 17-18, pp. 2132–2135, 2005.

[21] M. Okada, Y. Kita, T. Nakajima et al., "Evaluation of a novel vaccine (HVJ-liposome/HSP65 DNA + IL-12 DNA) against tuberculosis using the cynomolgus monkey model of TB," *Vaccine*, vol. 25, no. 16, pp. 2990–2993, 2007.

[22] M. Okada, Y. Kita, T. Nakajima et al., "Novel prophylactic and therapeutic vaccine against tuberculosis," *Vaccine*, vol. 27, no. 25-26, pp. 3267–3270, 2009.

[23] Y. Saeki, N. Matsumoto, Y. Nakano, M. Mori, K. Awai, and Y. Kaneda, "Development and characterization of cationic liposomes conjugated with HVJ (Sendai virus): reciprocal effect of cationic lipid for in vitro and in vivo gene transfer," *Human Gene Therapy*, vol. 8, no. 17, pp. 2133–2141, 1997.

[24] K. Miki, T. Nagata, T. Tanaka et al., "Induction of protective cellular immunity against *Mycobacterium tuberculosis* by recombinant attenuated self-destructing *Listeria monocytogenes* strains harboring eukaryotic expression plasmids for antigen 85 complex and MPB/MPT51," *Infection and Immunity*, vol. 72, no. 4, pp. 2014–2021, 2004.

[25] C. C. Dascher, K. Hiromatsu, X. Xiong et al., "Immunization with a mycobacterial lipid vaccine improves pulmonary pathology in the guinea pig model of tuberculosis," *International Immunology*, vol. 15, no. 8, pp. 915–925, 2003.

[26] I. Sugawara, T. Udagawa, S. C. Hua et al., "Pulmonary granulomas of guinea pigs induced by inhalation exposure of heat-treated BCG Pasteur, purified trehalose dimycolate and methyl ketomycolate," *Journal of Medical Microbiology*, vol. 51, no. 2, pp. 131–137, 2002.

[27] Y. Kita, M. Okada, T. Nakajima et al., "Development of therapeutic and prophylactic vaccine against Tuberculosis using monkey and transgenic mice models," *Human Vaccines*, vol. 7, pp. 108–114, 2011.

[28] H. McShane, A. A. Pathan, C. R. Sander et al., "Recombinant modified vaccinia virus Ankara expressing antigen 85A boosts BCG-primed and naturally acquired antimycobacterial immunity in humans," *Nature Medicine*, vol. 10, no. 11, pp. 1240–1244, 2004.

[29] H. A. Fletcher, A. A. Pathan, T. K. Berthoud et al., "Boosting BCG vaccination with MVA85A down-regulates the immunoregulatory cytokine TGF-β1," *Vaccine*, vol. 26, no. 41, pp. 5269–5275, 2008.

[30] M. Okada and Y. Kita, "Tuberculosis vaccine development: the development of novel (preclinical) DNA vaccine," *Human Vaccines*, vol. 6, no. 4, pp. 297–308, 2010.

[31] S. H. Kaufmann, G. Hussey, and P. H. Lambert, "New vaccines for tuberculosis," *The Lancet*, vol. 375, no. 9731, pp. 2110–2119, 2010.

[32] D. B. Lowrie, R. E. Tascon, V. L. D. Bonato et al., "Therapy of tuberculosis in mice by DNA vaccination," *Nature*, vol. 400, no. 6741, pp. 269–271, 1999.

[33] D. F. Hoft, "Tuberculosis vaccine development: goals, immunological design, and evaluation," *The Lancet*, vol. 372, no. 9633, pp. 164–175, 2008.

[34] U. D. Gupta, V. M. Katoch, and D. N. McMurray, "Current status of TB vaccines," *Vaccine*, vol. 25, no. 19, pp. 3742–3751, 2007.

[35] F. Tanaka, M. Abe, T. Akiyoshi et al., "The anti-human tumor effect and generation of human cytotoxic T cells in SCID mice given human peripheral blood lymphocytes by the in vivo transfer of the interleukin-6 gene using adenovirus vector," *Cancer Research*, vol. 57, no. 7, pp. 1335–1343, 1997.

[36] H. McShane, A. A. Pathan, and C. R. Sander, "Recombinant modified vaccinia virus Ankara expressing antigen 85A boosters BCG-primed and naturally acquired antimycobacterial immunity in humans," *Nature Medicine*, vol. 10, pp. 1240–1244, 2008.

[37] M. Tanaka, Y. Kaneda, S. Fujii et al., "Induction of a systemic immune response by a polyvalent melanoma-associated antigen DNA vaccine for prevention and treatment of malignant melanoma," *Molecular Therapy*, vol. 5, no. 3, pp. 291–299, 2002.

[38] S. Takeda, K. Shiosaki, Y. Kaneda et al., "Hemagglutinating virus of Japan protein is efficient for induction of CD4(+) T-cell response by a hepatitis B core particle-based HIV vaccine," *Clinical Immunology*, vol. 112, no. 1, pp. 92–105, 2004.

[39] G. Sakaue, T. Hiroi, Y. Nakagawa et al., "HIV mucosal vaccine: nasal immunization with gp160-encapsulated hemagglutinating virus of Japan-liposome induces antigen-specific CTLs and neutralizing antibody responses," *Journal of Immunology*, vol. 170, no. 1, pp. 495–502, 2003.

[40] Y. Kaneda, T. Nakajima, T. Nishikawa et al., "Hemagglutinating virus of Japan (HVJ) envelope vector as a versatile gene delivery system," *Molecular Therapy*, vol. 6, no. 2, pp. 219–226, 2002.

[41] Y. Kaneda, "New vector innovation for drug delivery: development of fusigenic non-viral particles," *Current Drug Targets*, vol. 4, no. 8, pp. 599–602, 2003.

[42] Y. Kaneda, S. Yamamoto, and T. Nakajima, "Development of HVJ Envelope Vector and Its Application to Gene Therapy," *Advances in Genetics*, vol. 53, pp. 307–332, 2005.

[43] M. Ito, S. Yamamoto, K. Nimura, K. Hiraoka, K. Tamai, and Y. Kaneda, "Rad51 siRNA delivered by HVJ envelope vector enhances the anti-cancer effect of cisplatin," *Journal of Gene Medicine*, vol. 7, no. 8, pp. 1044–1052, 2005.

[44] H. Mima, S. Yamamoto, M. Ito et al., "Targeted chemotherapy against intraperitoneally disseminated colon carcinoma using a cationized gelatin-conjugated HVJ envelope vector," *Molecular Cancer Therapeutics*, vol. 5, no. 4, pp. 1021–1028, 2006.

[45] A. M. Cooper, J. Magram, J. Ferrante, and I. M. Orme, "Interleukin 12 (IL-12) is crucial to the development of protective immunity in mice intravenously infected with *Mycobacterium tuberculosis*," *Journal of Experimental Medicine*, vol. 186, no. 1, pp. 39–45, 1997.

[46] K. M. Baek, S. Y. Ko, M. Lee et al., "Comparative analysis of effects of cytokine gene adjuvants on DNA vaccination against *Mycobacterium tuberculosis* heat shock protein 65," *Vaccine*, vol. 21, no. 25-26, pp. 3684–3689, 2003.

[47] E. Martin, A. T. Kamath, H. Briscoe, and W. J. Britton, "The combination of plasmid interleukin-12 with a single DNA vaccine is more effective than Mycobacterium bovis (bacille Calmette-Guèrin) in protecting against systemic *Mycobacterim avium* infection," *Immunology*, vol. 109, no. 2, pp. 308–314, 2003.

Microbiology and Immunology

Microbiol Immunol 2011; 55: 565–573
doi:10.1111/j.1348-0421.2011.00348.x

ORIGINAL ARTICLE

Decreased plasma granulysin and increased interferon-gamma concentrations in patients with newly diagnosed and relapsed tuberculosis

Nada Pitabut[1], Surakameth Mahasirimongkol[2], Hideki Yanai[3], Chutharut Ridruechai[1], Shinsaku Sakurada[4], Panadda Dhepakson[5], Pacharee Kantipong[6], Surachai Piyaworawong[7], Saiyud Moolphate[3], Chamnarn Hansudewechakul[8], Norio Yamada[9], Naoto Keicho[4], Masaji Okada[10], and Srisin Khusmith[1]

[1]Department of Microbiology and Immunology, Faculty of Tropical Medicine, Mahidol University, Bangkok, [2]Medical Genetic Section, National Institute of Health, Department of Medical Sciences, Ministry of Public Health, Nonthaburi, [3]TB/HIV Research Project, Research Institute of Tuberculosis, Japan Anti-Tuberculosis Association, Chiang Rai, [4]Department of Respiratory Diseases, Research Institute, National Center Global Health and Medicine, Kiyose, Tokyo, [5]Medical Biotechnology Center, National Institute of Health, Department of Medical Science, Ministry of Public Health, Nonthaburi, [6]Chiang Rai Hospital, Chiang Rai, [7]Mae Chan Hospital, Chiang Rai, [8]Chiang Rai Provincial Health Office, Chiang Rai, Thailand, [9]Research Institute of Tuberculosis, Japan Anti-Tuberculosis Association, Kiyose, Tokyo, and [10]Clinical Research Center, National Hospital Organization, Kinki-Chuo Chest Medical Center, Sakai, Osaka, Japan

ABSTRACT

Granulysin and interferon-gamma (IFN-γ) have broad antimicrobial activity which controls *Mycobacterium tuberculosis* (*M. tuberculosis*) infection. Circulating granulysin and IFN-γ concentrations were measured and correlated with clinical disease in Thai patients with newly diagnosed, relapsed and chronic tuberculosis (TB). Compared to controls, patients with newly diagnosed, relapsed and chronic TB had lower circulating granulysin concentrations, these differences being significant only in newly diagnosed and relapsed TB ($P < 0.001$ and 0.004, respectively). Granulysin concentrations in patients with newly diagnosed and relapsed TB were significantly lower than in those with chronic TB ($P = 0.003$ and $P = 0.022$, respectively). In contrast, significantly higher circulating IFN-γ concentrations were found in patients with newly diagnosed and relapsed TB compared to controls ($P < 0.001$). The IFN-γ concentrations in newly diagnosed and relapsed patients were not significantly different from those of patients with chronic TB. However, *in vitro* stimulation of peripheral blood mononuclear cells (PBMCs) from patients with newly diagnosed, relapsed and chronic TB with purified protein derivative (PPD) or heat killed *M. tuberculosis* (H37Ra) enhanced production of granulysin by PBMCs. *In vitro*, stimulation of PBMCs of newly diagnosed TB patients with PPD produced greater amounts of IFN-γ than did controls, while those stimulated with H37Ra did not. The results demonstrate that patients with active pulmonary TB have low circulating granulysin but high IFN-γ concentrations, suggesting possible roles in host defense against *M. tuberculosis* for these agents.

Key words clinical disease, granulysin, IFN-γ, tuberculosis.

Correspondence
Srisin Khusmith, Department of Microbiology and Immunology, Faculty of Tropical Medicine, Mahidol University, 420/6 Rajvithi Road, Bangkok 10400, Thailand.
Tel: +66 2 3549100-13 ext. 1594; fax: +66 2 6435583; email: tmskm@mahidol.ac.th

Received 2 February 2011; revised 19 April 2011; accepted 21 April 2011.

List of Abbreviations: APC, antigen presenting cell; BCG, Bacillus Calmette-Guérin; CTL, cytotoxic T lymphocyte; E, ethambutol; H, isoniazid; IFN-γ, interferon gamma; IGRA, interferon-γ release assay; IL, interleukin; MDR, multi-drugs resistance; MHC, major histocompatibility complex; *Mtb*, *Mycobacterium tuberculosis*, *M. tuberculosis*, *Mycobacterium tuberculosis*; NK, natural killer; PBMC, peripheral blood mononuclear cell; PPD, purified protein derivative; R, rifampicin; S, streptomycin; TB, tuberculosis; Th1, T-helper type 1; TMB, tetramethylbenzidine; TNF, tumor necrosis factor; TST, tuberculin skin test; XDR, extensively drug resistant; Z, pyrazinamide.

Tuberculosis is a major health problem worldwide, with one third of the world population being infected and approximately 1.1–1.7 million deaths annually (1). Most individuals infected with *Mtb* are asymptomatic. However, 5–10% will progress to active TB during their lifetime, the remainder being resistant to active TB, but remaining infected. Relapse of TB, which is defined as an episode of infection occurring after a previous episode has been treated and considered cured, is possibly due to endogenous reactivation when it occurs in geographical areas with a low incidence of TB infection (2). However, generally the risk of relapse depends on the intensity of exposure to *Mtb*. Other factors that directly affect the clinical course of TB are host factors, including age, immune status, genetic factors and coinfection with HIV, and bacterial factors, including degree of exposure, virulence of strain, MDR and XDR.

Protective immunity against *Mtb* infection involves activated macrophages, antigen-specific T cells and type-1 cytokines such as IL-12, IFN-γ and TNF (3, 4). Inherited defects of the IL-12/IFN-γ pathway appear to result in a variety of changes in mycobacterial susceptibility. People with genetic deficiencies in the type-1 cytokine (IL-12/IL-23/IFN-γ) axis, and those with neutralizing autoantibody against IFN-γ, have been found to be highly susceptible to mycobacterial infections including TB (5–8). In active pulmonary TB, these effectors of the immune response are activated, as evidenced by observation of high circulating IFN-γ concentrations that decrease significantly following two months of therapy (9, 10).

Granulysin can kill extracellular *Mtb* directly, or intracellular bacteria in the presence of perforin (11), expression of granulysin in CD8+T cells being induced upon activation. It has recently been reported that granulysin is strongly associated with diverse activities of NK cells and CTLs in physiological and pathological settings, and might be a useful novel serum marker for evaluating the overall status of host cellular immunity (12). In patients with cutaneous leprosy, the frequency of granulysin-expressing T cells lesions is 6-fold greater than in those with the disseminated lepromatous form of the disease (13). In contrast, adults with active pulmonary TB in a highly TB endemic area in Indonesia had significantly lower plasma granulysin concentrations than did controls, these concentrations increasing after 2 months of anti-TB therapy to values similar to those of controls, and having increased even further after completion of anti-TB therapy. These changes in granulysin concentrations occurred predominantly in patients in whom IFN-γ negative T cells were expressed, suggesting that in TB the cellular sources of IFN-γ and granulysin are partly non-overlapping (14). Similar findings have been reported for Italian children, the lowest concentrations having been found in TB patients who were PPD negative at the time of diagnosis (15), indicating the involvement of granulysin and IFN-γ in curative immune responses against *Mtb*. In chronic pulmonary TB, lung tissue biopsy has shown reduction in amounts of perforin and granulysin in relation to granzyme A, while higher per cell expression of perforin and granulysin is associated with bacteriological control, suggesting that perforin and granulysin could be used as markers or correlates of immune protection in human TB (16). However, effective host mechanisms against *Mtb* infection are not well understood, this lack of understanding being a problem in regard to vaccine development and immunotherapy for TB. Moreover, so far there is limited information regarding the roles of IFN-γ and granulysin in recurrent TB. Therefore, the present study aimed to investigate whether granulysin and IFN-γ responses are associated with clinical disease in patients with newly diagnosed, relapsed and chronic pulmonary TB in northern Thailand, where TB is endemic.

MATERIALS AND METHODS

Subjects

One hundred and fifty-five pulmonary TB patients (aged 9 to 88 years) were recruited from the outpatient and inpatient clinics of Chiang Rai Hospital and Mae Chan Hospital, in the north of Thailand. These included 102 male and 53 female patients with newly diagnosed and previously treated pulmonary TB. Patients with extrapulmonary TB and pulmonary TB/HIV seropositive were excluded. All patients with pulmonary TB had clinical symptoms and a confirmed diagnosis on the basis of presence of acid-fast bacilli in sputum on microscopic examination, positive cultures of *Mtb*, medical history and chest radiographic findings. Patients were categorized according to World Health Organization criteria (1), which include ascertaining whether the patient has previously received TB treatment. The TB drug regimens were based on the recommendations of the National Tuberculosis Program, Ministry of Public Health, Thailand. Standard TB treatment drugs consist of streptomycin (S), isoniazid (H), rifampicin (R), pyrazinamide (Z) and ethambutol (E). In this study, patients with newly diagnosed TB were defined as those who had never received treatment for TB or had taken anti-TB drugs for less than 1 month prior to enrollment ($n = 84$). Patients with relapsed TB were defined as those previously treated for TB and declared "cured" or "treatment completed", and currently diagnosed as *Mtb* positive by smears and cultures ($n = 35$). Patients with chronic TB were defined as those who had started on a retreatment regimen after having failed previous treatment ($n = 36$). No patients had been reported to be MDR or

XDR cases on the basis of drug sensitivity tests at the time of enrollment in this study.

Thirty three healthy individuals (aged 21 to 54 years old, median = 36 years) recruited from the Blood Bank of Chiang Rai Hospital, Mae Chan Hospital and Phan Hospital were used as controls. They had no history suggestive of TB or other acute infectious diseases or diabetes at the time of enrollment. However, they were not subject to chest X-rays, TSTs or testing for latent TB infection and infection manifesting as active TB by IGRA upon enrollment.

The ethical aspects of this study were approved by the Ethical Review Committee for Research in Human Subjects, Ministry of Public Health, Thailand (Ref. No.3/2550) as part of a project studying multiple factors in recurrent TB, and written informed consent was obtained from all subjects.

Blood samples

Before instituting anti-TB therapy, blood was collected aseptically in EDTA Vacutainers. Plasma and packed cells were separated by centrifugation and stored at −80°C.

HIV screening

HIV positive cases were excluded from the study by screening with the particle agglutination assay (Serodia-HIV-1/2, Fujirebio, Tokyo, Japan) and/or immunochromatographic rapid test (Determine HIV-1/2, Abbott Laboratories, Champaign, IL, USA) or by ELISA (Enzygnost Anti-HIV 1/2 plus ELISA, Dade Behring, Marburg, Germany).

Peripheral blood mononuclear cells isolation and stimulation

Peripheral blood mononuclear cells from 75 pulmonary TB patients and 4 healthy controls were isolated by Ficoll-Hypaque density gradient centrifugation. In brief, 3 mL of whole blood in K_3EDTA (Greiner Bio-One, Bangkok, Thailand) was diluted with an equal volume of PBS, mixed gently and layered carefully over 3 mL Ficoll-paque PLUS (Amersham Biosciences, Uppsala, Sweden). After centrifugation at 1000 g for 20 min at room temperature, the PBMCs were harvested. The supernatant was removed after centrifugation at 700 g for 10 min at 4°C and the pellet adjusted with RPMI 1640 containing 10% FBS. The viable PBMCs were counted in 0.2% Trypan blue. Approximately 1×10^6 PBMCs/mL in RPMI 1640 medium containing 10% FBS and 2-mercapto ethanol were added to each well of a 24 well plate, stimulated either with 20 μg/mL of PPD (Japan BCG laboratory, Kiyose, Japan) or heat killed *Mtb* (H37Ra) (Difco, Detroit, MI, USA) and incubated at 37°C in 5% CO_2. The supernatants were harvested after 40 hr of stimulation, centrifuged at 1200 g for 3 min at 4°C and kept at −80°C. PMBCs stimulated with 20 μg/mL of PPD and not stimulated were used as positive and negative controls, respectively.

Determination of circulating granulysin and granulysin production by peripheral blood mononuclear cell stimulation assay

The granulysin concentrations in plasma and stimulated PBMC supernatant were determined by ELISA according to the manufacturer's instructions (BD Biosciences Pharmingen, San Diego, CA, USA). The tests were done in duplicate. Briefly, a microtiter plate (Costar, Cambridge, MA, USA) was coated with 100 μL/well of 5 μg/mL monoclonal mouse anti-human granulysin (clone RB1) (MBL International, Nagoya, Japan) in 0.05 M carbonate-bicarbonate buffer (pH 9.5) overnight at 4°C. The plates were washed with PBS containing 0.05% Tween 20 and blocked with buffered protein solution with ProClin-150 at room temperature for 1 hr. After being washed, the undiluted plasma was added and incubated for 2 hr at room temperature. The bound antigens were detected with 0.1 μg/mL of monoclonal mouse anti-human granulysin biotin (RC8) (MBL International) and avidin-horseradish peroxidase (Av-HRP) conjugate (BD Biosciences Pharmingen) diluted to 1:1000. After incubation for 1 hr, the reactions were developed by coloring with TMB substrate (BD Biosciences Pharmingen) for 20 min in the dark. The reaction was stopped by 2N H_2SO_4 solution (BD Biosciences Pharmingen). Optical densities were measured at 450 nm wavelength by an ELISA reader (ELx808 IU ultra microplate reader, Bio-Tek instruments, Winooski, VT, USA). Granulysin concentrations were calculated from a standard curve using granulysin containing culture supernatant obtaining from Cos7 cell transfected with gene encoding 15K granulysin. The lower detection limit for granulysin was 0.047 ng/mL.

Determination of circulating interferon-γ concentrations and interferon-γ production from stimulated mononuclear cells *in vitro*

Interferon-γ concentrations in plasma and stimulated PBMC supernatant were determined by ELISA according to the manufacturer's instruction (BD Biosciences Pharmingen). The tests were done in duplicate. Briefly, a microplate (Costar) was coated with 100 μL/well of anti-human IFN-γ (diluted to 1:250 in 0.1 M sodium carbonate) and incubated overnight at 4°C. The plates were washed three times with PBS containing 0.05% Tween 20, blocked with 200 μL/well of buffered protein solution with ProClin-150 and incubated at room temperature for 1 hr. After being washed, 100 μL of undiluted sample was added and incubated for 2 hr at room temperature. The bound